SWITCHING MODE POWER SUPPLY NOISE SOURCE IMPEDANCE MEASUREMENT AND EMI FILTER CHARACTERIZATION

by

Dongbing Zhang

Thesis submitted to the Faculty of the
Virginia Polytechnic Institute and State University
in partial fulfillment of the requirements for the degree of

MASTER OF SCIENCE

in

Electrical Engineering

Approved by:

Dr. Dan Y. Chen, Chairman

Dr. Fred C. Lee

Dr. Dan M. Sable

September, 1996

Blacksburg, Virginia

Key Words: EMI, filter, noise, source impedance, power supply, characterization

SWITCHING MODE POWER SUPPLY NOISE SOURCE IMPEDANCE MEASUREMENT AND EMI FILTER CHARACTERIZATION

by

Dongbing Zhang

Committee Chairman: Dan Y. Chen

Electrical Engineering

(ABSTRACT)

The effectiveness of an EMI filter is closely related to the impedance of the noise source. Due to the time-varying nature of the noise source impedance of an off-line power supply, the measurement of it cannot be done using conventional impedance measuring methods. Two new methods, the insertion loss method and the signal injection method, are proposed to perform such a measurement. The insertion loss method utilizes the EMI emission as a signal source and derives the source impedance by measuring the emission attenuation caused by an inserted impedance. The signal injection method injects a signal to the power supply and measures the response. The insertion loss method is verified experimentally both for common mode and differential mode. The signal injection method for common mode source impedance measurement is experimentally verified. That for differential mode source impedance

measurement requires a faster equipment and is not fully verified.

An EMI filter is usually characterized in the manufacturer's catalog by its attenuation in a standard system (50Ω source impedance and 50Ω load impedance). The effectiveness of the filter in a practical system may significantly deviate from the manufacturer's data. To provide the users with practically useful information, a scheme to characterize the EMI filter, the impedance matrix approach is proposed. This approach takes parasitic effect into consideration and the parameters can be measured relatively easily. The approach is verified experimentally by applying a commercial EMI filter to a power supply and comparing the predicted attenuation with the measured one.

To My Parents

ACKNOWLEDGMENTS

I want to express my sincere thanks to my advisor, Dr. Dan Y. Chen, without whose constant encouragement, helpful instructions and active involvement the completion of this thesis and the NASA STTR project on which it is based would not be possible.

I would like to thank Dr. Dan M. Sable of Virginia Power Technologies, INC, who was the project manager, for his continuous encouragement and trust during the process of the project, and for his time and effort to serving in my graduate committee.

I would like to thank Mr. Mark Nave of the EMC Services, who was the principal investigator in the above mentioned project, for his many knowledgeable and helpful hints and patient discussions in solving the many problems encountered during the entire process of the project.

I would like to thank Dr. Fred Lee for his time and effort serving in my graduate committee, and especially for the opportunity he provided me to work as a research assistant at VPEC.

My thanks also go to the NASA Small Business Technology Transfer Program, without whose financial support, this project would never have happened.

Last but not least, I want to thank my wife, who gave birth to our daughter, and my parents-in-law for their understanding, patience and great help in daily life.

TABLE OF CONTENTS

TABLE OF FIGURES

LIST OF ABBREVIATIONS

CM: common mode

CMRR: common mode rejection ratio

DM: differential mode

DUT: device under test

ILM: insertion loss method

LISN: line impedance stabilization network

RWB: resolution bandwidth

SA: spectrum analyzer

SIM: signal injection method

VBW: video bandwidth

X CAPACITOR: a capacitor that connects line and neutral wires

Y CAPACITOR: one of a pair of capacitors that connect line/neutral and ground

Z_s: Noise Source Impedance of a Power Supply

Chapter I

INTRODUCTION

Electromagnetic interference (EMI) design has always been a serious concern for power electronic engineers. It affects not only the EMI performance of the circuit but also the size and the cost of the system. It is fair to say that EMI design often determines if a product can be successfully introduced to the market in a timely fashion.

The performance of an EMI filter depends not only on the filter itself but also the noise source and load impedance. Fig. 1-1 illustrates this assertion. In both Fig. 1-1(a) and (b), the same filter is used for different source impedance (Z_s) and load impedance (Z_l) conditions, and the filter attenuations are drastically different, as shown by Fig. 1-1(c). In EMI measurements, the load impedance is that of a standardized network known as the Line Impedance Stabilization Network (LISN) and is therefore always known. The source impedance, however, varies among different circuits and is usually unknown. This fact has two implications for the designers.

(1) In general, without knowing the noise source impedance, it is difficult to design an effective EMI filter.

(2) If an off-the-shelf commercial filter is the choice, the catalog attenuation data given traditionally for a filter is meaningless because in reality, the effectiveness of the

filter depends on source impedance which varies from one power supply to another.

It is the intention of this thesis to address these two issues. They will be discussed separately in the following.

1.1 Measurement of Noise Source Impedance

Schneider [1] proposed a method to measure Z_s in off-line converters. The method relies on the resonance between an adjustable load inductor or capacitor and the noise source. There are several drawbacks in that approach. First, it is difficult to build adjustable inductors and capacitors. Second, the dependency on resonance makes it difficult to go beyond 1MHz. Third, the source impedance has to be assumed of first order, i.e., either capacitive or inductive.

In this thesis, two new methods to measure Z_s are proposed and experimentally verified. The first approach is the Insertion Loss Method (ILM). In the Insertion Loss Method, the magnitude of Z_s can be easily measured by measuring the attenuation of an inserted series or shunt impedance component. The phase of Z_s can then be derived by the Hilbert transform. The concept of insertion loss method is not new, but it's the first time being proposed and implemented to deal with the source impedance issue of a switching power supply. The second proposed approach is based on external signal injection and is named the Signal Injection Method (SIM) by the author. Experiments to implement these two methods are proposed and verified in this thesis. Both methods are good up to a fairly high frequency and are easy to apply.

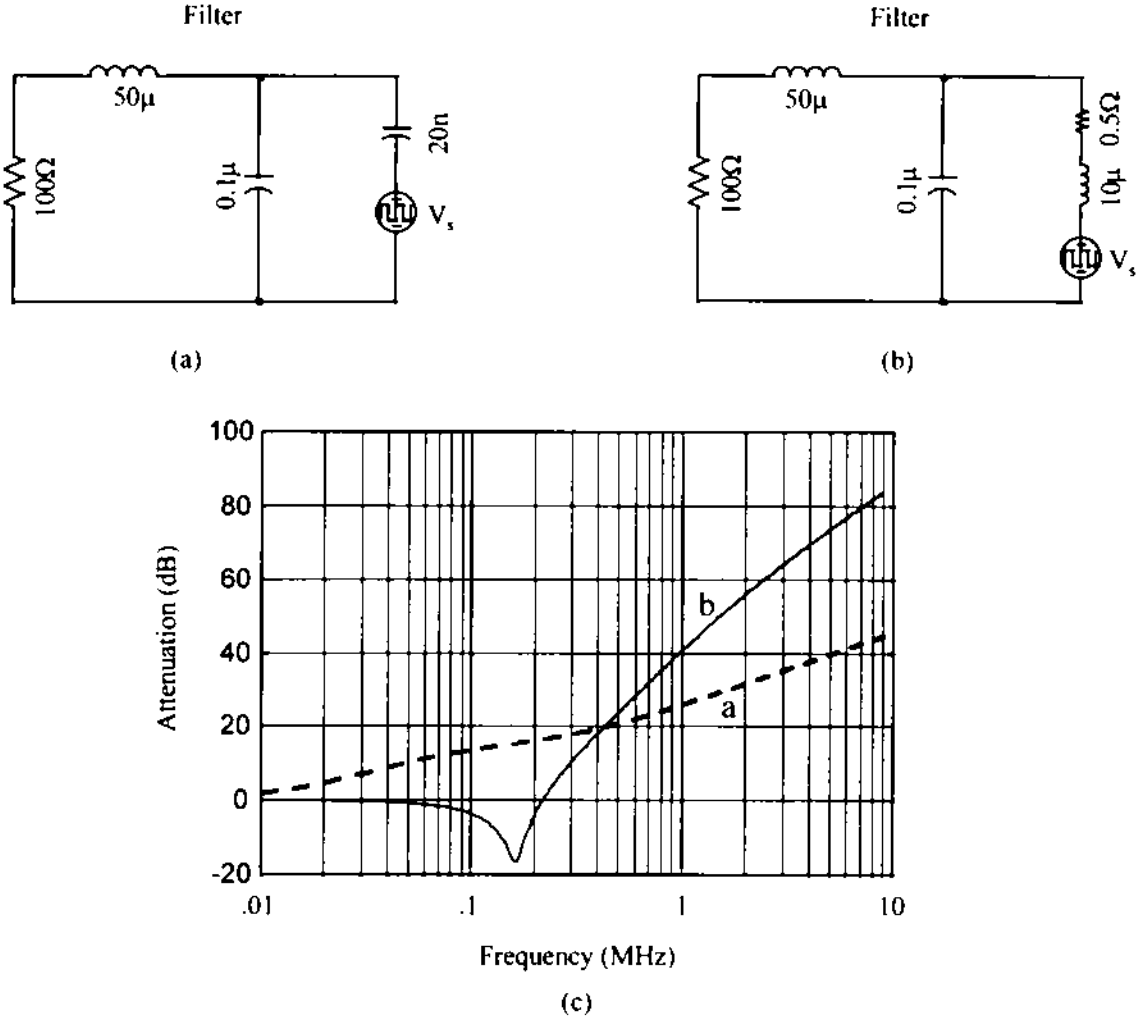

Fig. 1-1 Attenuation of the Same LC Filter with Different Source Impedance

1.2 Characterization of EMI Filters

Another topic in this thesis is the characterization of an EMI filter, especially a commercial EMI filter. Up to date, all commercially available EMI filters are characterized by filter attenuation curves published in the manufacturers' catalogs. However, these attenuation curves are obtained with a 50Ω system, i.e. both the source and the load impedance are assumed 50Ω resistive. In reality, the source and load impedance of the circuit under test can be very much different from 50Ω and therefore, the manufacturers' published attenuation curves could deviate significantly from reality. In the past, due to the lack of knowledge of the noise source impedance, further effort to characterize these filters was not very meaningful. However, as it becomes easier to obtain the noise source impedance information, prediction of filter effectiveness becomes practical.

A new method is proposed and implemented in this thesis to characterize EMI filters. Instead of characterizing the filter by attenuation curves as conventionally done, it is proposed the filter be described by its impedance matrix. This can be done without having to assume the values of source and load impedance. From the measured impedance matrix and given source and load impedance, the filter attenuation curves can be readily calculated. The parameters of the proposed method can be obtained experimentally with common equipment.

1.3 Difference between Source Impedance Z_s and Input Impedance Z_i

The meanings of the two impedances, Z_s and Z_i are totally different. Z_i is related to the control issue and Z_s is related to the EMI issue of a power supply. Within the control bandwidth, Z_i can have a negative real part while Z_s is always passive. Regardless of the difference in meaning, however, the measurement technique of Z_i used in practice may seem applicable to Z_s measurement. As will be explained in Section 3.2.1 on page 31, the approach used to measure Z_i is not suitable for the measurement of Z_s due to high frequency considerations.

In this thesis, Chapter II briefly reviews some of the issues involved in conducted EMI measurements. Chapter III introduces the two new methods to measure Z_s. Issues related to Hilbert transform and time-varying Z_s measurement are also discussed. Measurement results using both methods are shown and verified. An off-line switching power supply was used in the experimental verification. Both methods were used and the results were compared. In Chapter IV, the method of using the impedance matrix to describe an EMI filter is introduced. The reason for choosing impedance matrix rather than other types of describing matrices is also discussed. The impedance matrix of a commercial EMI filter is measured and its usefulness is verified by the agreement between the predicted and measured attenuations. Chapter V concludes the thesis. Future research areas are also suggested.

Chapter II

CONDUCTED EMI MEASUREMENTS

In this chapter, a brief review of conducted EMI measurement is given. Then several special issues are discussed in Sections 2.3, 2.4 and 2.5. These issues are closely related to the experimental results to be described in later chapters.

2.1 Conducted EMI Measurement Setup

The setup for conducted EMI measurement is represented in Fig. 2-1. Inside the dotted box is a Line Impedance Stabilization Network (LISN). The LISN is used to provide a fixed noise load to the DUT so that the difference between test sites is inconsequential. The 60Hz power signal can pass through the LISN without being impeded, whereas the high frequency EMI signals are highly damped. The two 1KΩ resistors are called bleeding resistors and are used to discharge the capacitors after use for safety reasons. Two BNC connectors are connected to the two 1KΩ resistors and are called RF ports. Measurement of EMI emissions is made at one of the two RF ports of the LISN. The two RF ports are always terminated with 50Ω resistors, either a dummy load or the input impedance of a spectrum analyzer. In Fig. 2-1, the upper RF port (LINE side) is

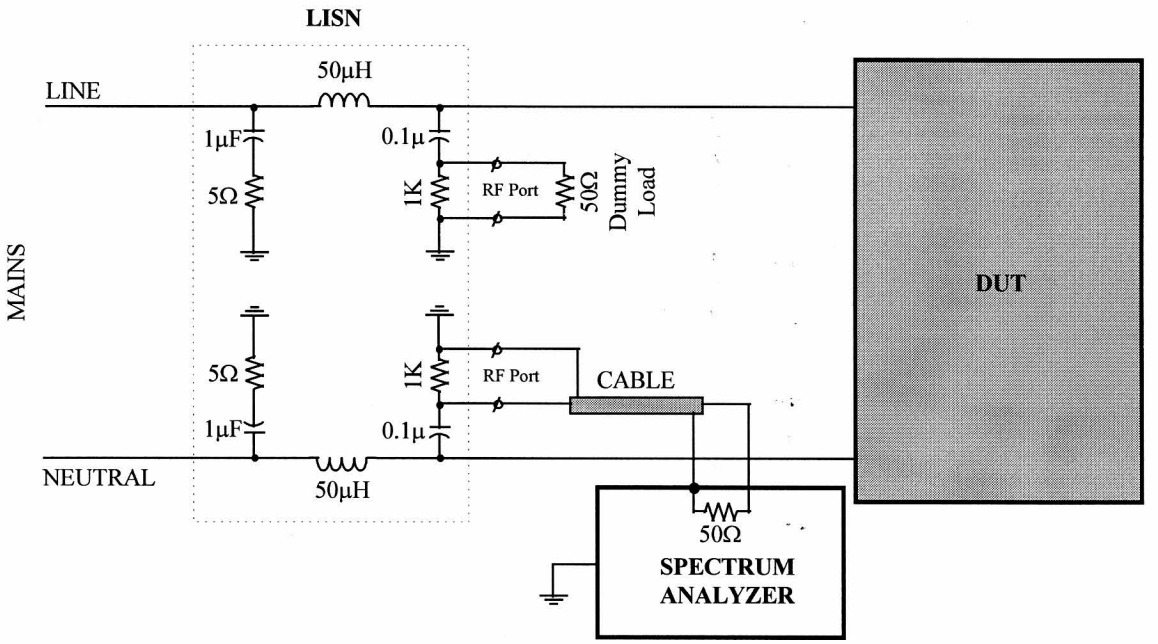

Fig. 2-1 Conducted EMI Measurement Using A LISN

terminated with the dummy load while the lower RF port (NEUTRAL side) is connected to a spectrum analyzer. Since the input impedance of the spectrum analyzer channel is 50Ω, the right two legs of the LISN are thus equally terminated.

2.2 Separation of Emission Modes by Power Combiners

Although separation of noise emission into common mode (CM below) and differential mode (DM below) is not required by regulatory agencies, it plays an important role in the EMI filter designing process. This is because CM signal is pure noise whereas DM contains the useful (and huge) 60Hz power signal as well as noise. This makes CM noise much more easily filtered than DM due to a much reduced inductor size.

The definition of CM and DM voltages or currents is explained in Fig. 2-2. The currents I_1 and I_2 are called total currents because they represent the real noise currents flowing in the two wires. The two 50Ω resistors represent the two noise paths provided by the LISN (refer to Fig. 2-1 also). The CM current and voltage are defined as:

$$I_{CM} = \frac{1}{2} \cdot (I_1 + I_2) \qquad (1)$$

$$V_{CM} = \frac{1}{2} \cdot (V_1 + V_2) \qquad (2)$$

and the DM current and voltage are defined as:

$$I_{DM} = \frac{1}{2} \cdot (I_1 - I_2) \qquad (3)$$

$$V_{DM} = \frac{1}{2} \cdot (V_1 - V_2). \qquad (4)$$

A device called 'the noise separator' has been reported which can be used to

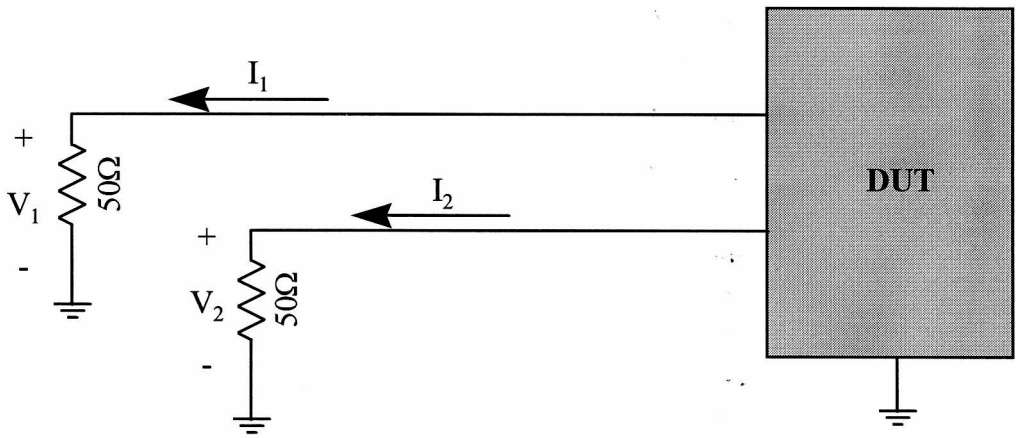

Fig. 2-2 Simplified Noise Emission Pattern

separate the CM and DM noise [2] and will be used in later chapters. The portion of the noise separator that rejects CM and passes DM is called the DM detector. The portion which rejects DM and passes CM is called the CM detector. It should be pointed out that the two types of detectors have limited rejection of the mode they are supposed to reject. Rejection ability is usually described by rejection ratio which is obtained by dividing the signal appearing at the input end by that appearing at the output end. It shall be helpful to later discussions to define two terms here:

CM Residual: CM signal appearing at the output end of a DM detector.

DM Residual: DM signal appearing at the output end of a CM detector.

2.3 Broadband Signals and Narrowband Signals

There are three basic EMI noise classes: narrowband, broadband and random [3]. Distinguishing between noise classes is very important in terms of EMI filter design. The regulatory requirements on different noise classes are usually different. The way to suppress noises of different classes is also different.

A periodic signal is considered broadband if its fundamental frequency (and hence the harmonic pitch) is much lower than the designated resolution bandwidth (RBW) setting of a spectrum analyzer (SA below) so that no individual sinusoidal components can be discerned. Otherwise the signal is considered narrowband, also known as continuous wave or sinewave.

From the definition, it is clear that whether a periodic signal is broadband or nar-

rowband depends on the RBW setting. Since a periodic signal's harmonic pitch is equal to its fundamental frequency, when the signal has a very low fundamental frequency compared to the RBW, the resolution bandwidth filter of a SA will pass numerous harmonics and if the peak detector is used, the summed effect will be displayed. This makes the originally very small but closely spaced harmonics appear as a relatively huge harmonic. Since the broadband signal in the time domain is a series of sparsely spaced pulses, even if its total energy within a resolution bandwidth is comparable to that of a narrowband signal, the former is less a nuisance in broadcasting. The use of a quasi-peak detector by the FCC regulations serves the purpose of distinguishing the two types of signals by greatly damping the broadband signals.

In an off-line converter, the broadband noise is usually caused by the interruption of LISN inductor currents when the input rectifier turns off. The LISN currents end up charging the LISN capacitors, causing differential mode impulses with a 120Hz pulse repetition rate.

EMC regulations sometimes have a relaxed requirement on broadband signals. The degree of relaxation depends on the pulse repetition rate of the broadband signal.

A signal can be identified as a broadband signal if it meets the following criteria.

1) Number of harmonics increases when sweep time of the SA increases, and vice versa.

2) Magnitudes of harmonics decrease when RBW of the SA decreases.

3) Magnitudes of harmonics decrease when Video Bandwidth (VBW) of the SA

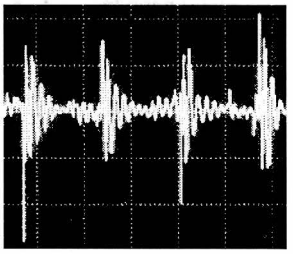

(a) Time Domain Waveform
Scale: 5ms/div, 10mv/div

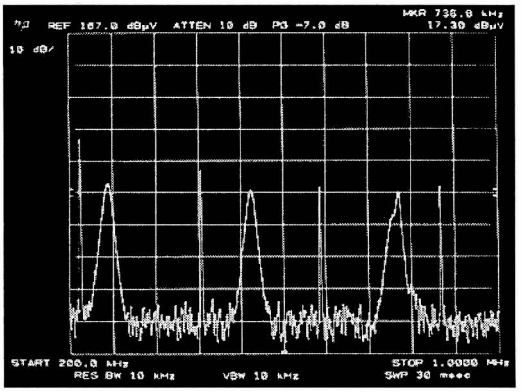

(b) Spectrum With Sweep Time = 30ms

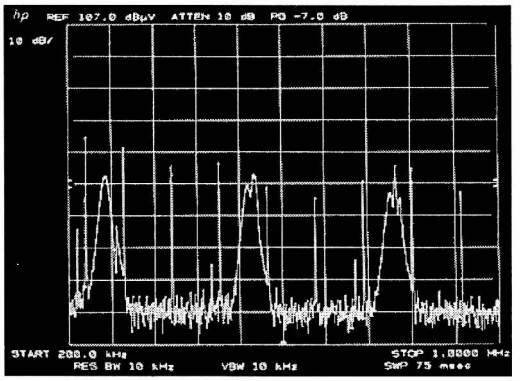

(c) Spectrum With Sweep Time = 75ms

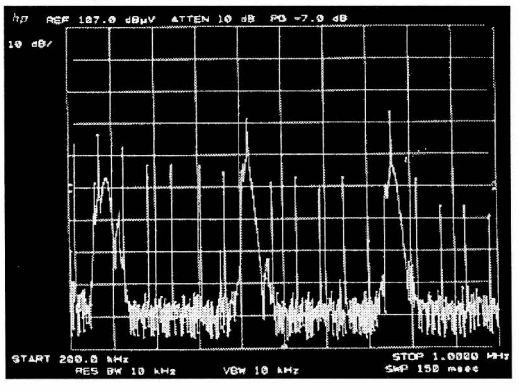

(d) Spectrum With Sweep Time = 150ms

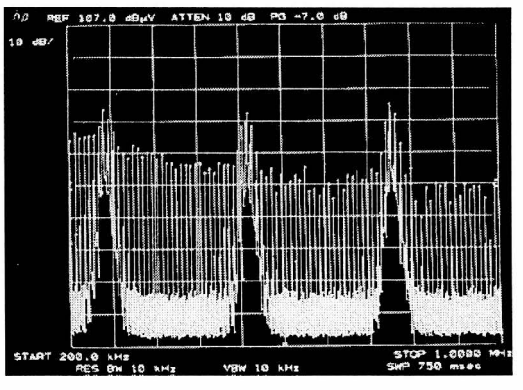

(e) Spectrum With Sweep Time = 750ms

Fig. 2-3 Broadband Versus Narrowband Signals

decreases.

No narrowband signals meets any of the above descriptions.

As an illustration, Fig. 2-3 shows some pictures describing a situation when narrowband and broadband signals are mixed. It can be seen in (a) that there are huge pulses repeating at 120Hz. When a SA is used to measure the signal, different results can be obtained with different setting of the sweep time. In (b), three harmonics of the narrow band signal are clearly recognizable. There are only four occurrences of broadband spikes. The time between two adjacent spikes is equal to the time between two adjacent pulses in (a). As the sweep time increases, the narrowband harmonics remain unchanged but the broadband spikes become more and more closely spaced, as can be seen in (c), (d) and (e). Notice that sometimes the highest peak of the broadband spikes in the spectrum far exceeds those of the narrowband harmonics and this may result in a false measurement when using a peak detector without distinguishing the two classes of signals.

Understanding of this section should help interpret the measurement results to be discussed in Section 3.3.

2.4 Zero-Span Mode of a Spectrum Analyzer

Zero-Span is a special mode of operation of a SA because the SA stays at a fixed point on the frequency axis and displays signal power around that frequency only.

In the Zero-Span mode, a SA behaves similarly to an oscilloscope, i.e. the abscissa

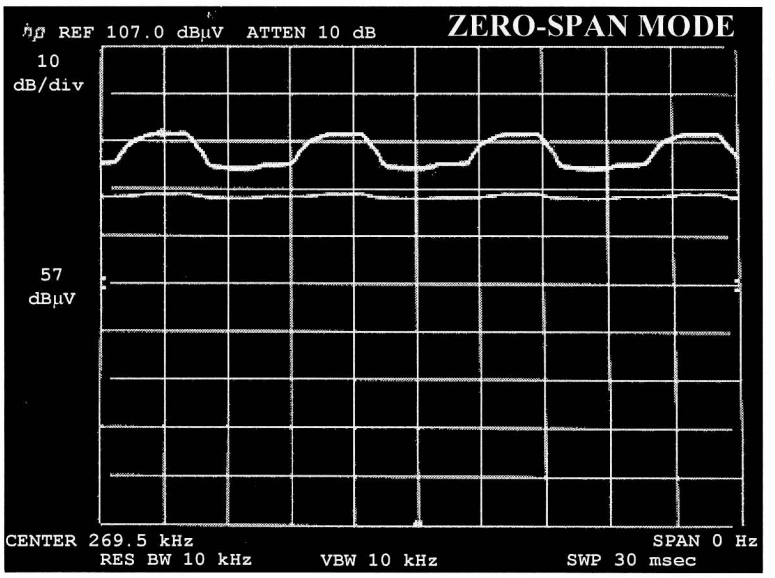

Fig. 2-4 A Zero-Span Screen
time base: 3ms/div

represents time instead of frequency. The major difference between the two is the RBW filter of the SA is a band pass filter whereas the filter in an oscilloscope is usually a low pass filter. Of course, the SA usually detects and displays only the peak of the time-domain signal at the output of the RBW filter, while the oscilloscope displays instantaneous values.

Zero-Span is sometimes a more convenient way to look at amplitude-modulated signals when the modulating signal is of very low frequency. This will be further explained in the next section.

As an illustration, Fig. 2-4 shows a zero-span screen. The SA is not sweeping on the frequency axis but rather stays at the center frequency (269.5KHz in the figure). What is displayed is signal amplitude versus time. If the signal is a continuous wave, its zero span should appear a flat line. That the upper trace in Fig. 2-4 is not a flat line indicates the amplitude is being modulated. It can be told from the picture that the frequency of the modulating signal is approximately 120Hz. Zero-span feature of a SA will be used to observe the emission of an amplitude modulated signal in Section 2.5.

2.5 Amplitude-Modulated Harmonics

Since a switching power supply is a non-linear circuit, magnitudes of harmonics are sometimes modulated. This is especially true when an off-line (non-PFC) converter is concerned. The diode bridge in the off-line converter turns on and off at 120Hz, making the impedance of the noise path alternate at the same frequency. For an amplitude-

modulated signal, its harmonics change amplitude with each sweep when 'free-run' trigger mode is chosen.

As an example, Fig. 2-5 shows an off-line flyback converter whose conducted emissions are being measured. Fig. 2-6 shows the zero-span picture at the specified frequency (269.5KHz) of three signals. The highest trace is CM emission, the middle trace is DM emission, and the lowest trace is the attenuated DM emission when an X-impedance (1μF in series with a 1Ω resistor) is inserted. The four flat tops in the CM trace, each lasting about 1.6ms, are found to coincide with diode bridge ON period. So the zero-span of the fundamental CM component tells us that the CM emission is higher when the diode bridge is on, and lower when off. Notice that the DM emission (middle trace) seems to be the opposite. This will be explained further in Section 3.3.

Since the modulating frequency is 120Hz, it would not be possible to discern the sideband harmonics with a 10KHz RBW. Under a much lower RBW (10Hz, for example), it is possible that the modulated signal be resolved into sidebands but the frequency of the carrier has to be very stable, otherwise the spectrum would appear polluted. In the context of EMI emission measurement, zero-span is a good way to examine amplitude-modulated harmonics generated by an off-line converter.

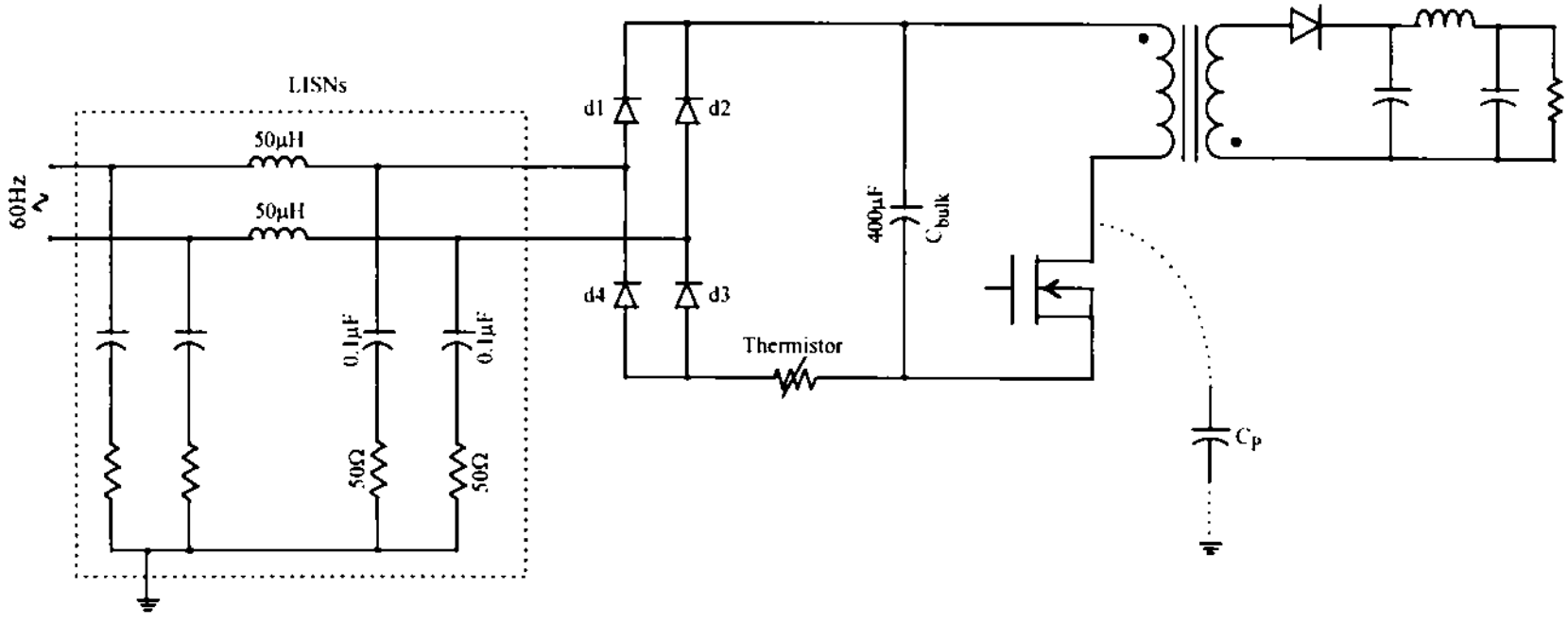

Fig. 2-5 Measuring Conducted Emissions Of An Off-Line Flyback Converter

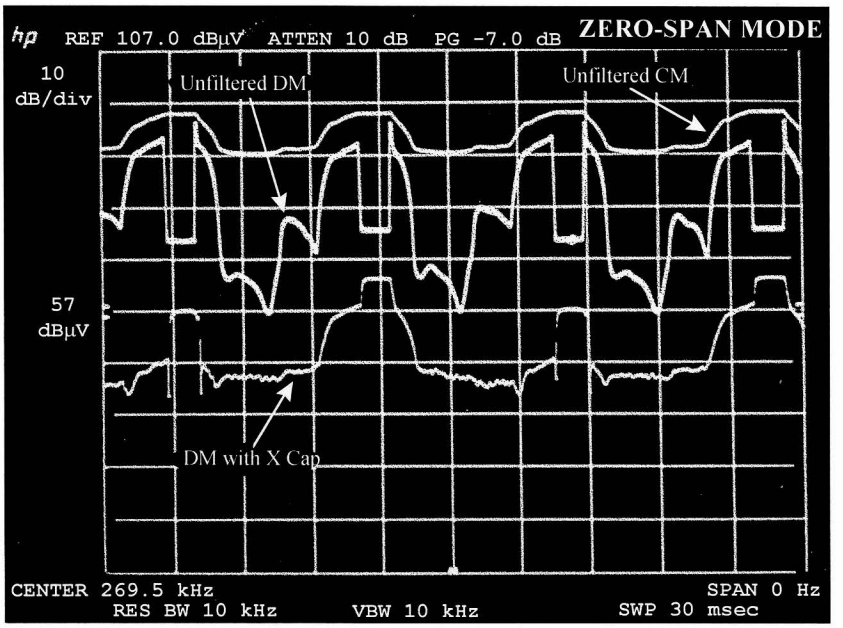

Fig. 2-6 Zero-Span Diagram of CM Emission, DM Emission and Attenuated DM Emission

Chapter III
MEASUREMENT OF NOISE SOURCE IMPEDANCE

In this chapter, two methods to measure the noise source impedance (Z_s) are proposed: the Insertion Loss Method and the Signal Injection Method. Both methods will be described in detail in the first two sections. It is to be noted that the measurement of noise source impedance is carried out while the power supply is in an operating condition. Issues of interpreting the measurement results pertinent to off-line power supplies are addressed in Section 3.3. It is found that the diode bridge of an off-line power supply can cause severe unbalance in the circuit and introduce significant DM noise during diode bridge OFF time. The conclusion is to totally ignore the DM source impedance during diode bridge OFF time. Experimental verification using an off-line switching power supply will be covered in Section 3.4.

3.1 Insertion Loss Method to Measure Source Impedance

The concept of noise source impedance is based on the simplified noise emission pattern shown in Fig. 3-1. The DUT (noise generating circuit such as a power supply) is reduced to a one-port network (whose impedance is the Z_s) and the LISN is represented by a resistor R_{load}. An EMI filter is then reduced to a two-port network that is inserted

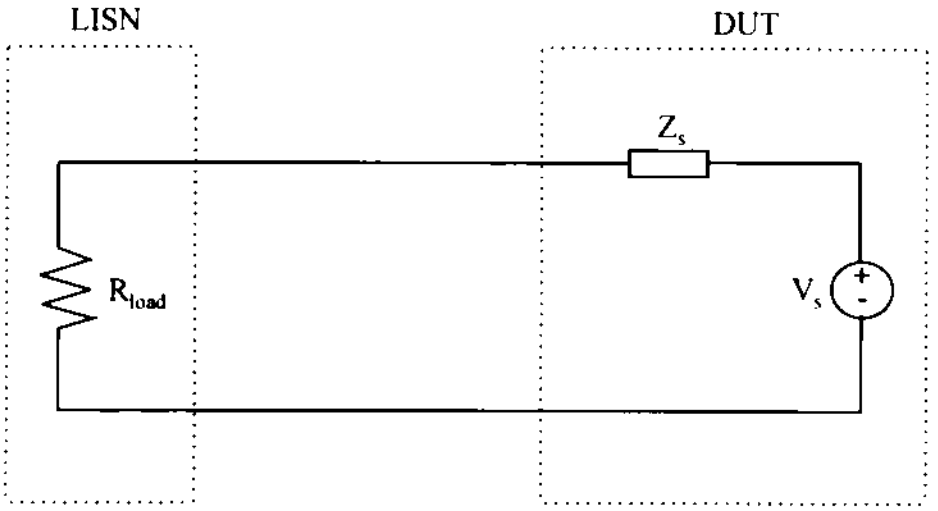

Fig. 3-1 Simplified Noise Emission Pattern

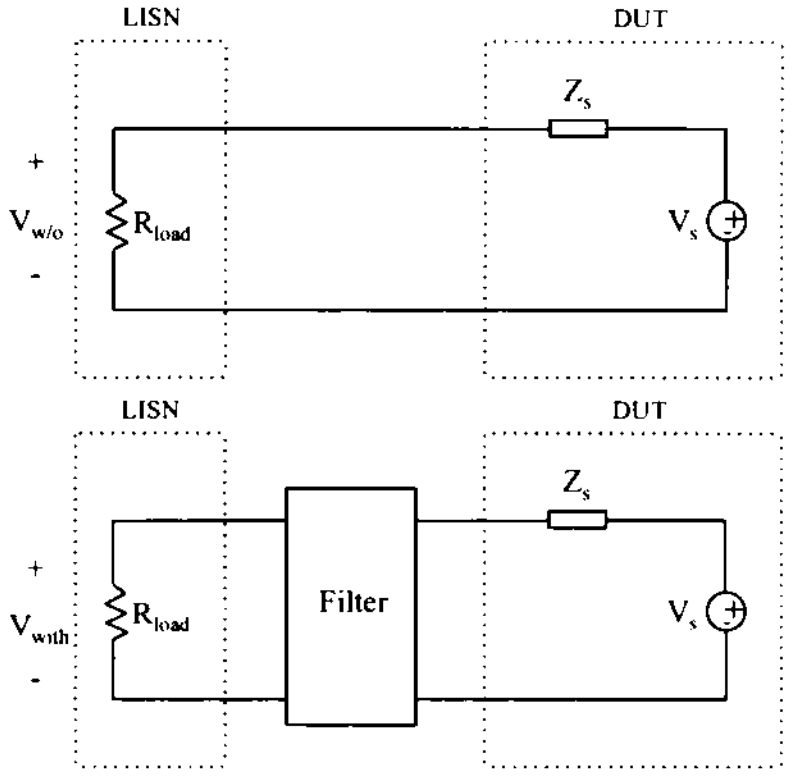

Fig. 3-2 Simplified Noise Emission Pattern

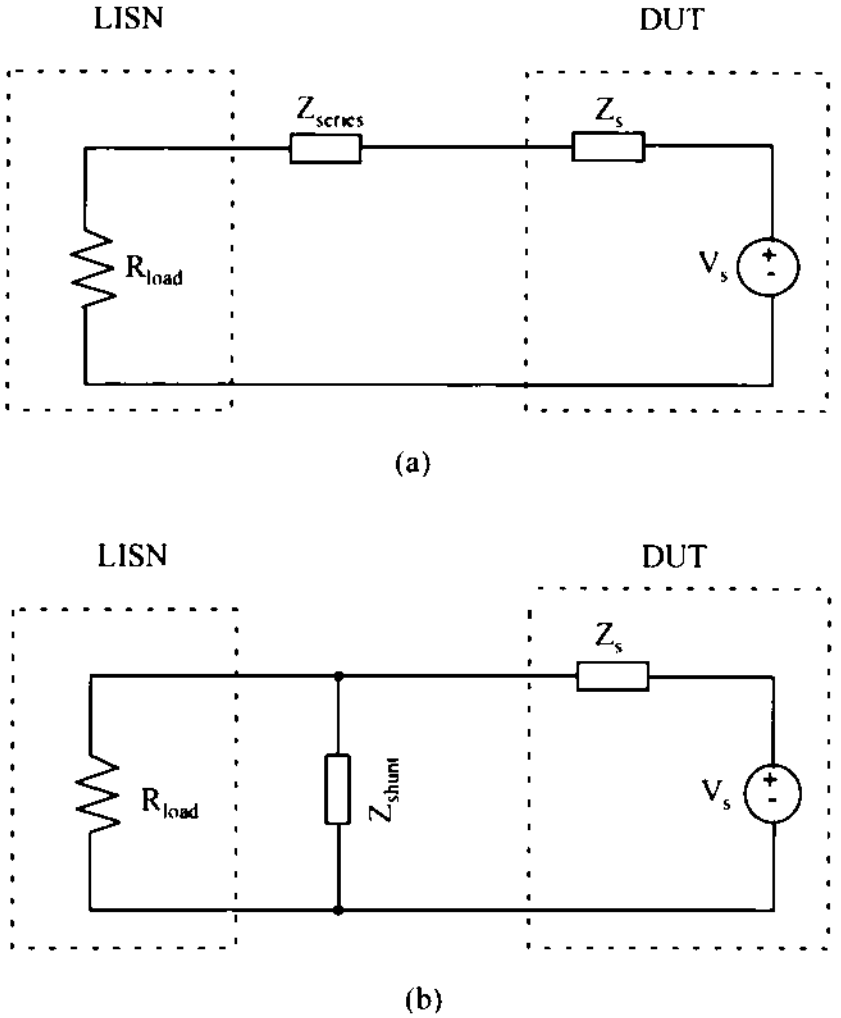

Fig. 3-3 Deriving $|Z_s|$ by the Insertion Loss Method

(a) series insertion method (b) shunt insertion method

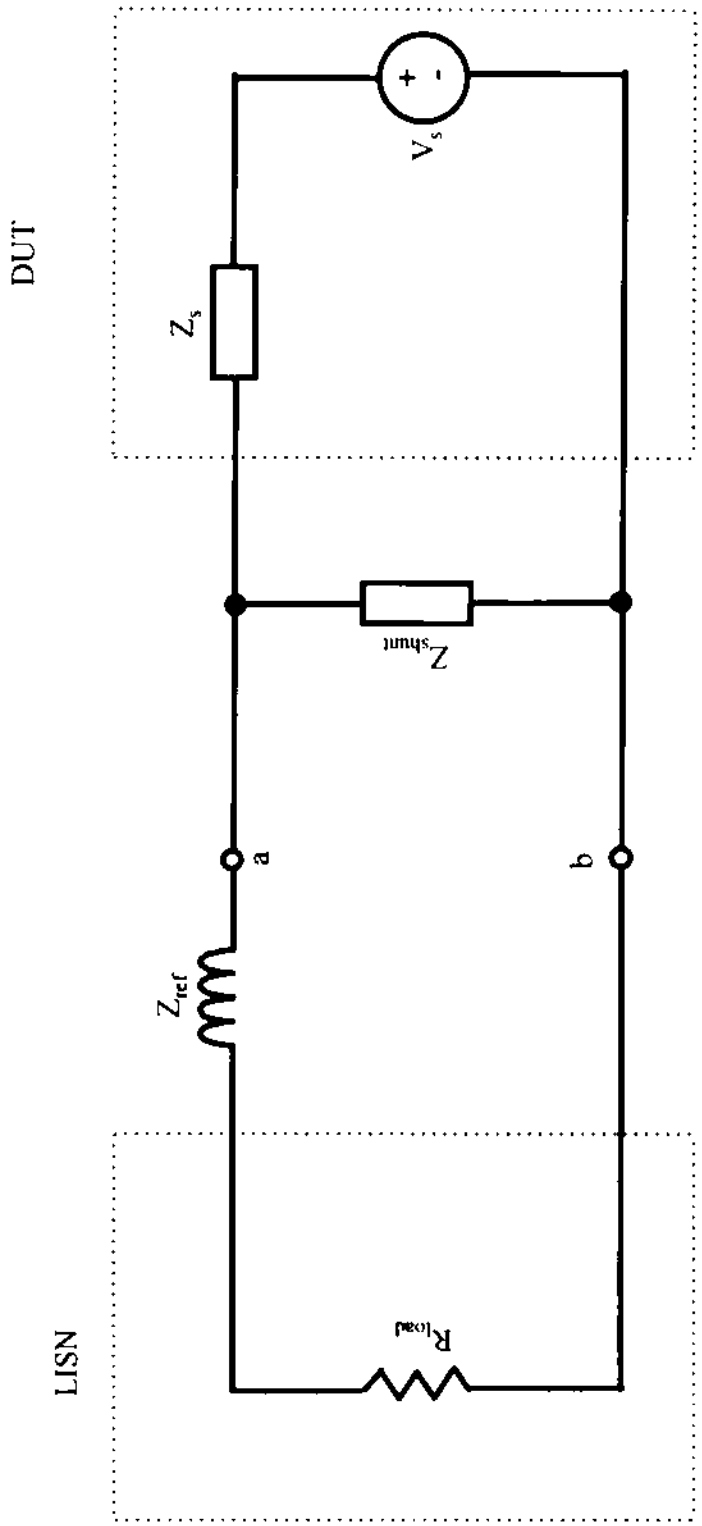

Fig. 3-4 Use of a Reference Filter

in between the DUT and the LISN, see Fig. 3-2. The idea of Insertion Loss Method (ILM) is very simple. Referring to Fig. 3-3, if a piece of filter element (either Z_{series} or Z_{shunt}) is inserted between Z_s and R_{load}, the noise voltage across R_{load} will change (usually reduced). This change is measured by insertion loss (or attenuation) A which is defined as the ratio of voltages across R_{load} before and after the filter element is inserted, see Fig. 3-2 and the equation below.

$$A = \frac{V_{w/o}}{V_w} \qquad (5)$$

It is noted that the insertion loss is a complex number in general, although usually only the magnitude is measured. From the measured insertion loss and the impedance of the inserted filter element, the magnitude of the source impedance $|Z_s|$ can be directly calculated as described in the following section.

3.1.1 Measurement of Magnitude of Source Impedance

When obtaining $|Z_s|$, either series insertion method or shunt insertion method is used, depending on the relative magnitude of $|Z_s|$ versus R_{load}. Three cases are discussed in the following.

CASE I. $\quad |Z_s| >> R_{load}$

In such a case, the series insertion method is used (see Fig. 3-3(a)). By inserting a series component, the expression for attenuation can be simplified as follows:

$$A = \frac{\frac{R_{load}}{R_{load}+Z_s}\times V_S}{\frac{R_{load}}{R_{load}+Z_s+Z_{series}}\times V_S} = 1 + \frac{Z_{series}}{R_{load}+Z_s}. \qquad (6)$$

Since $|Z_s| >> R_{load}$ is assumed, Eq.(6) becomes:

$$A = 1 + \frac{Z_{series}}{Z_s}. \qquad (7)$$

From Eq.(7) we have,

$$\big||A|-1\big| \le \left|\frac{Z_{series}}{Z_s}\right| \le |A|+1, \qquad (8)$$

where $|Z_{series}|$ is given, and $|A|$ is obtained through attenuation measurement.

Since $\frac{Z_{series}}{Z_s}$ can take any phase angle, the best estimate for its magnitude, when no knowledge of the phase angle is assumed, is the geometric mean of the two boundaries of its magnitude:

$$\left|\frac{Z_{series}}{Z_s}\right| \approx \sqrt{\big||A|-1\big| \times \big(|A|+1\big)} = \sqrt{\big||A|^2-1\big|} \qquad (9)$$

In other words,

$$|Z_s| \approx \frac{|Z_{series}|}{\sqrt{\big||A|^2-1\big|}} \qquad (10)$$

Obviously, the larger the insertion loss is, the more accurate Eq.(10) will be. This equation will be used later in Section 3.4 for finding the source impedance of a power supply.

CASE II. $|Z_s| << R_{load}$

In such a case, the shunt insertion method is used (see Fig. 3-3(b)). By inserting a shunt component, the expression for attenuation can be simplified as follows:

$$A = \frac{\frac{R_{load}}{R_{load}+Z_s}\times V_S}{\frac{R_{load}//Z_{shunt}}{R_{load}//Z_{shunt}+Z_s}\times V_S} = 1 + \frac{R_{load}//Z_s}{Z_{shunt}} \qquad (11)$$

Since $|Z_s| << R_{load}$ is assumed, Eq.(11) becomes:

$$A = 1 + \frac{Z_s}{Z_{shunt}}. \qquad (12)$$

Similar to *CASE I*, $|Z_s|$ can be best estimated as the following provided no knowledge of the phase of $\frac{Z_{series}}{Z_s}$ is assumed:

$$|Z_s| \approx |Z_{shunt}| \times \sqrt{|A|^2 - 1}, \qquad (13)$$

where again $|Z_{shunt}|$ is given and $|A|$ is obtained through attenuation measurement.

CASE III. $|Z_s|$ *and* R_{load} *of Comparable Magnitude*

Should such a case occur, R_{load} can be decreased or increased so that either CASE I or CASE II is satisfied. A better approach is to use a reference filter so that the LISN inductors and capacitors do not form a limitation to the noise load impedance (the 50μH LISN inductor limits the highest R_{load} value and the 0.1μF LISN capacitor limits how low R_{load} can be). A typical reference filter in the shunt insertion method is an inductor. See Fig. 3-4. The baseline emission is measured with Z_{ref} in place. When Z_{ref}

is made much greater than Z_s, the attenuation of the voltage between nodes a and b caused by Z_{shunt} is given by Eq.(12). Since the noise load is always R_{load} + Z_{ref}, the attenuation seen by R_{load} is also given by the same equation.

Similarly, series insertion method is also applicable. Instead of using a series impedance as the Z_{ref}, a shunt impedance much lower than the source impedance can be used to decrease the load impedance. Apparently, Eq.(10) is the right formula to use now.

It may be unclear that without first knowing $|Z_s|$, how does one know whether CASE I or CASE II above is true. The answer is to make a trial measurement first. When the series insertion method is applied, $|R_{load} + Z_s|$ can be found by Eq.(6). If the $|R_{load} + Z_s|$ turns out to be much greater than R_{load}, then CASE I must be true. Similarly, when the shunt insertion method is used, $|R_{load}//Z_s|$ can be found by Eq.(11). If the measured $|R_{load}//Z_s|$ is much less than R_{load}, then CASE II must be true.

3.1.2. Deriving Phase Information Using Hilbert Transform

Z_s is a complex function of frequency in general. The magnitude of Z_s can be found by either Eq.(10) or Eq.(13), as described above. But the phase of Z_s cannot be found from the same equations. In many applications, the information of phase angle of Z_s is inconsequential. In case the phase is desired, Hilbert transform can be used to derive it [4]. Hilbert transform basically establishes a relationship between the phase $\angle Z_s(\omega)$ and magnitude $|Z_s(\omega)|$ of a minimum phase function such as the impedance function [4],

see Eq.(14).

$$\angle Z_s(\omega) = \frac{2\omega}{\pi}\int_0^\infty \frac{|Z_s(\xi)| - |Z_s(\omega)|}{(\xi+\omega)(\xi-\omega)}d\xi \qquad (14)$$

As long as the magnitude function $|Z_s(\omega)|$ is known over a fairly wide frequency range (e.g. $0 \sim f_{max}$), the phase function $\angle Z_s(\omega)$ can usually be known quite accurately at least up to $f_{max}/3$. A theoretical example is given in the following to illustrate the point.

A linear and time invariant one-port network as shown in Fig. 3-4 is to be used as an example. Suppose the magnitude of the input impedance of the circuit is known only up to 20MHz, as shown in Fig. 3-5. The rest of the magnitude curve is guessed by the dotted straight line.

By applying the algorithm proposed in [4], phase can be derived over the same frequency range and is shown in Fig. 3-6 as the broken curve. It can be seen that the derived and actual phases match quite well in this example.

In a practical situation, the order of the system is never known. That is, the number of poles and zeros beyond the maximum measured frequency is not known.. This may bring the doubt that although each pole or zero contributes little to the low frequency phase, how does one know that there shall not be enough of them to have significant contribution to the low frequency phase? If that is the case, then the unaccounted for high frequency poles and zeros may become a uncontrollable source of error to the phase below the maximum measured frequency. Fortunately, for a passive impedance, the difference between the number of poles and the number of zeros can

never exceed one otherwise the impedance is no longer passive. This ensures that the contributions of high frequency poles and zeros to low frequency phase tend to cancel and the error caused is negligible.

3.2 Signal Injection Method To Measure Source Impedance

By using the signal injection method, a signal is injected externally to the DUT, and the response of the DUT is measured. The source impedance of the one-port network is calculable from the measured response. There are numerous ways to measure impedance. Some methods are more restricted than others as to the situations to which they can be applied. Among all those methods, the I-V method is the most straightforward and is widely used by impedance analyzers. However, it is to be pointed out that the I-V method is not a suitable way to measure the noise source impedance, when the switching power supply (DUT) is in operating condition. The more flexible V-V method is proposed as the appropriate implementation of the Signal Injection Method.

3.2.1 A Quick Review of I-V Method and V-V Method

Fig. 3-8 shows the simplified conceptual diagram of the I-V method. The voltage (V) and current (I) at the one-port terminals are measured and the source impedance is equal to the ratio V/I, provided the source voltage V_s is very small compared to injected signal V_{inject}. When V_s is significant, measurement is feasible with the help of a tracking generator, so that the harmonics of the noise source can be avoided. The I-V

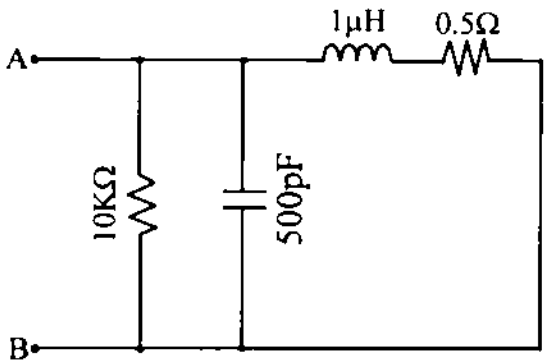

Fig. 3-5 A LTI One-Port Network

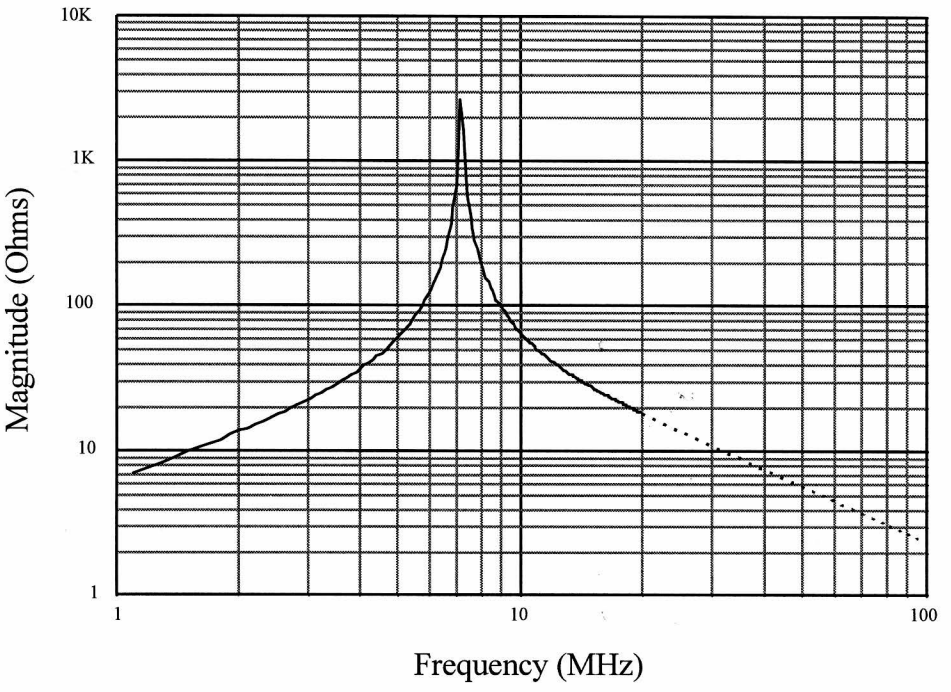

Fig. 3-6 Magnitude Plot of the Network in the Previous Figure

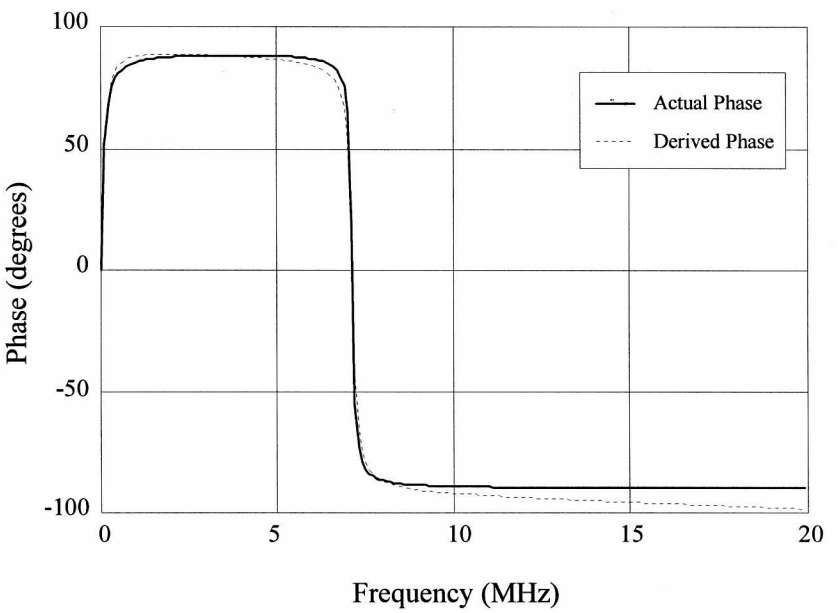

Fig. 3-7 Actual Phase and Hilbert Transform Derived Phase

approach is typically employed by an impedance analyzer whose probe has only two terminals. To have reasonable accuracy, the I-V method requires the use of either a high impedance voltage meter or a low impedance current sensor. This may bring problems, especially at high frequencies when impedance matching becomes critical. Another potential problem for the I-V method in the context of source impedance measurement is it measures the parallel combination of the noise load (typically LISN) and source impedance. The details will be covered in next section.

An alternative is the V-V method. Fig. 3-9 shows the conceptual diagram for V-V method. The two resistors R_1 and R_2 represent the impedance of the measuring voltmeters and are usually 50Ω. Since the voltage across Z_s is the sum of the voltages across R_1 and R_2 and the current flowing through Z_s is the same as that in R_2, the expression for Z_s is thus:

$$Z_s = \frac{V_1 - V_2}{V_2 / R_2} = R_2 \cdot \left(\frac{V_1}{V_2} - 1 \right). \qquad (15)$$

Since the voltages V_1 and V_2 can be easily measured as vector quantities, the phase of Z_s is known automatically. Again, V_1 is either assumed to be much smaller than V_{inject} or, when a tracking generator is used, to be of different frequency than V_{inject}.

The V-V method can be implemented by using a gain-phase analyzer. An advantage of the V-V method is no high impedance voltmeter is needed. The 50Ω vector voltmeters in the gain-phase analyzer are good enough.

It is to be noted that although the measurement of input impedance of a power

supply also employs the V-V method, there is an important difference in implementation. That is, a high impedance voltage probe is always used to measure V_1, see Fig. 3-9. The high impedance probe ceases to be of high impedance at high frequencies and tend to load down the measured circuit. It is also difficult to avoid signal distortions by using a high impedance probe at high frequencies due to transmission line impedance mismatch.

3.2.2 V-V Method Instead of I-V Method

Due to the nonlinear nature of the DUT, it is desirable to measure the source impedance with the DUT operating. In order to apply the Signal Injection Method, the noise source model is still assumed to be that in Fig. 3-1. The I-V method is rather limited here because the network (typically LISN's) supplying 60Hz power to the DUT tends to load down the source impedance and thus impose often a severe limitation on the highest measurable Zs. See Fig. 3-10. The impedance measured by the I-V setup is the parallel combination of Z_{net} and Z_s. Unless Z_{net} is much larger than Z_s, the measurement result deviates from Z_s significantly. The V-V method, on the other hand, shows an advantage in such a case due to its 'three point measurement'. See Fig. 3-11. Apparently, the presence of the 60Hz power source network does not affect the implementation of this method. For this reason, V-V method was chosen for this thesis work. The discussion hereafter is focused on this method.

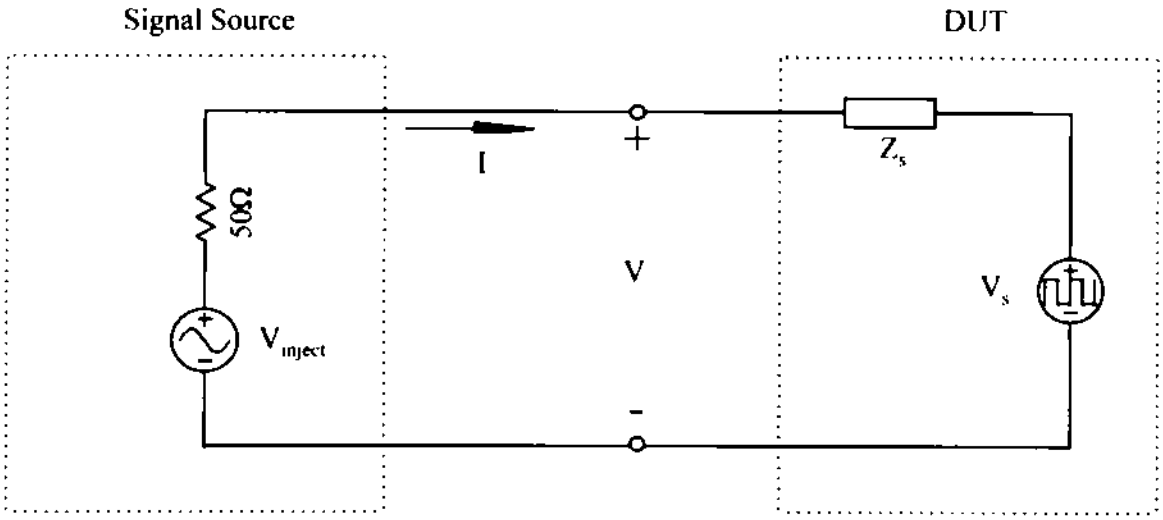

Fig. 3-8 Use I-V Method to Measure Z_s

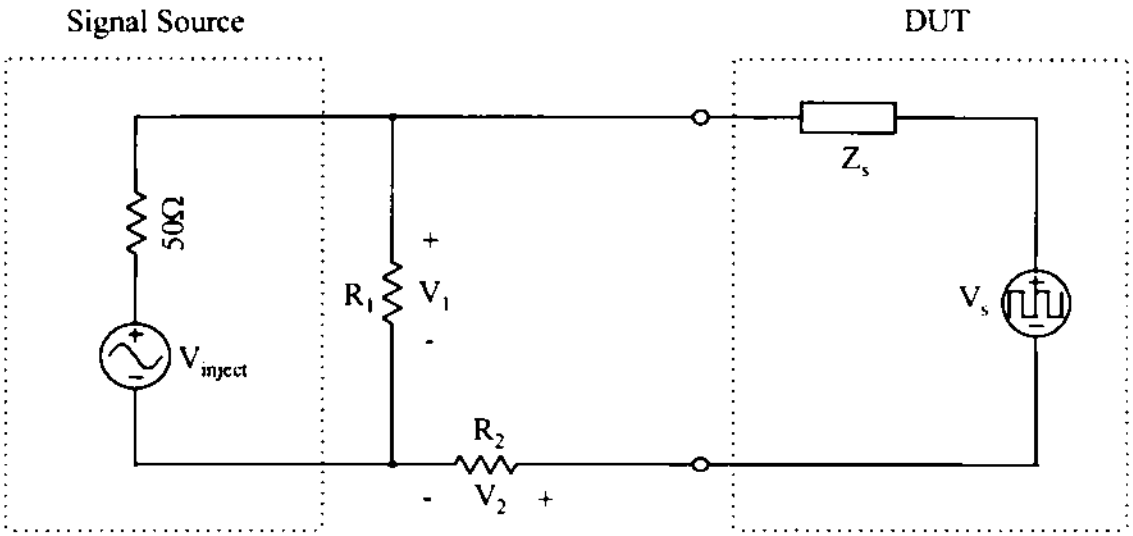

Fig. 3-9 Use V-V Method to Measure Z_s

3.2.3 *Measurement Setup of V-V Method*

To implement the V-V method, an HP4194A gain-phase analyzer is used. Fig. 3-12 shows the measurement setup for DM source impedance and Fig. 3-13 shows that for the CM source impedance. The dotted boxes represent signal injection source and vector voltmeters. The two 50Ω resistors R_1 and R_2 represent the input impedance of the two voltmeters. Wherever necessary, capacitors (C_1, C_2, and C_3) are used to isolate the signal source and voltmeters from the 60Hz power signal. Transformers are used to eliminate the grounding problem. Transformers are so designed that the magnetizing inductance appears to be a much higher impedance to the 50Ω termination resistance within the interested frequency range, so that the total termination resistance remains approximately 50Ω. The leakage inductance of the transformers should also be kept at a minimum to ensure that all the voltages appearing at the primary windings drop on the 50Ω resistors. In Fig. 3-12, the 500μH inductor and capacitor C_3 (1μF) are used to provide protection from 60Hz signal for the voltmeter (whose impedance is R_2). In Fig. 3-13, a common mode choke is used to bypass the 60Hz power signal (which is differential) so that it does not flow through the 50Ω resistor (R_2) of one of the two voltmeters. Notice the choice of values of the magnetizing inductance and capacitance is based on the interested frequency range. If the frequency range is too broad, it is necessary to break up the range into subranges and use different set of component values for different subranges.

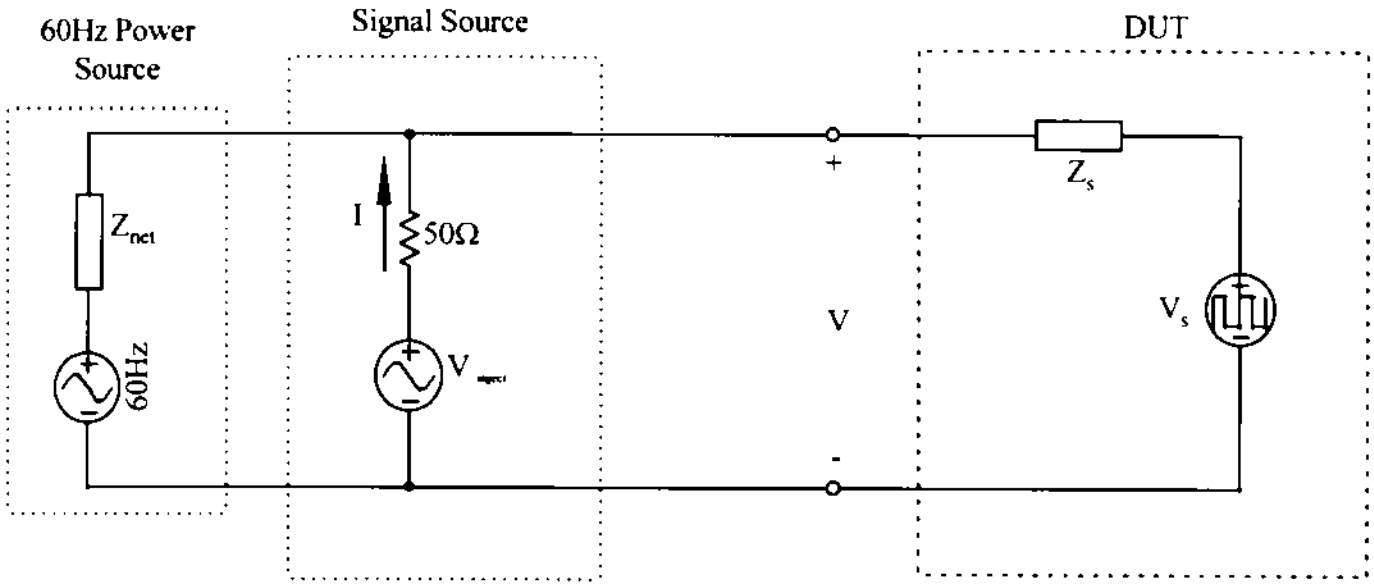

Fig. 3-10 Difficulty in Applying I-V Method

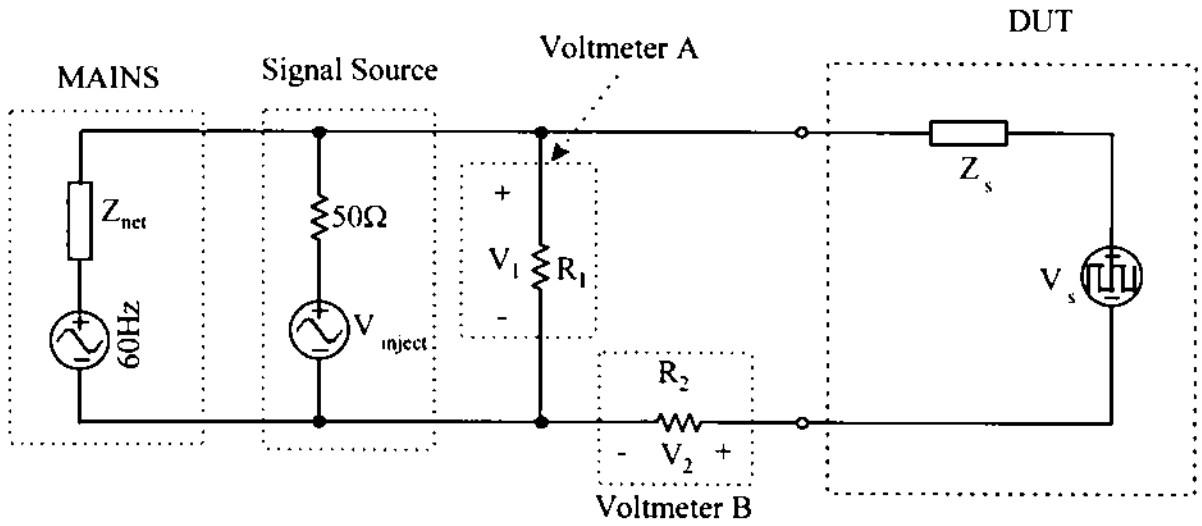

Fig. 3-11 V-V Method Is Not Affected by 60Hz Power Network

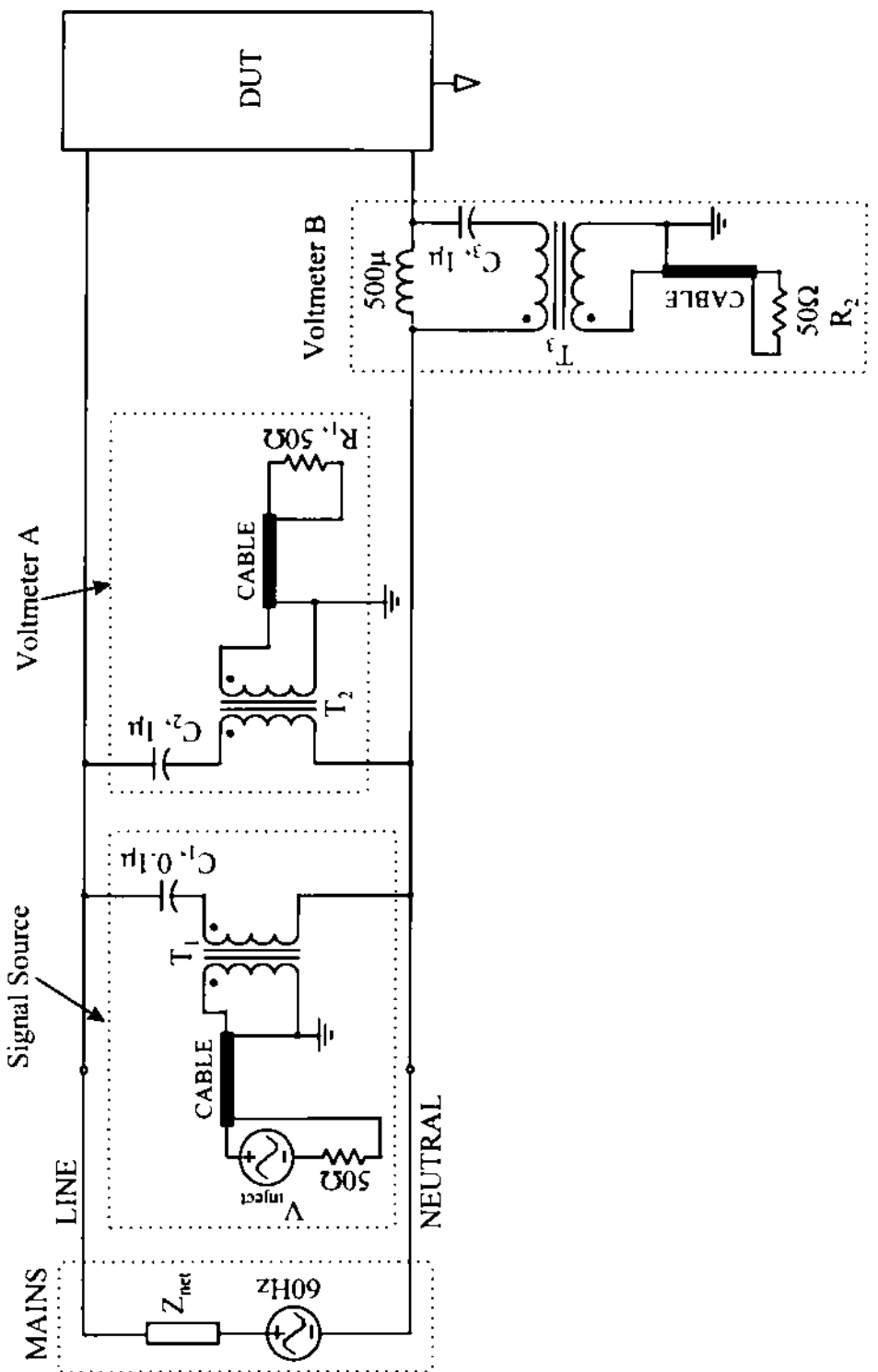

Fig. 3-12 Z_{sdm} Measurement Setup

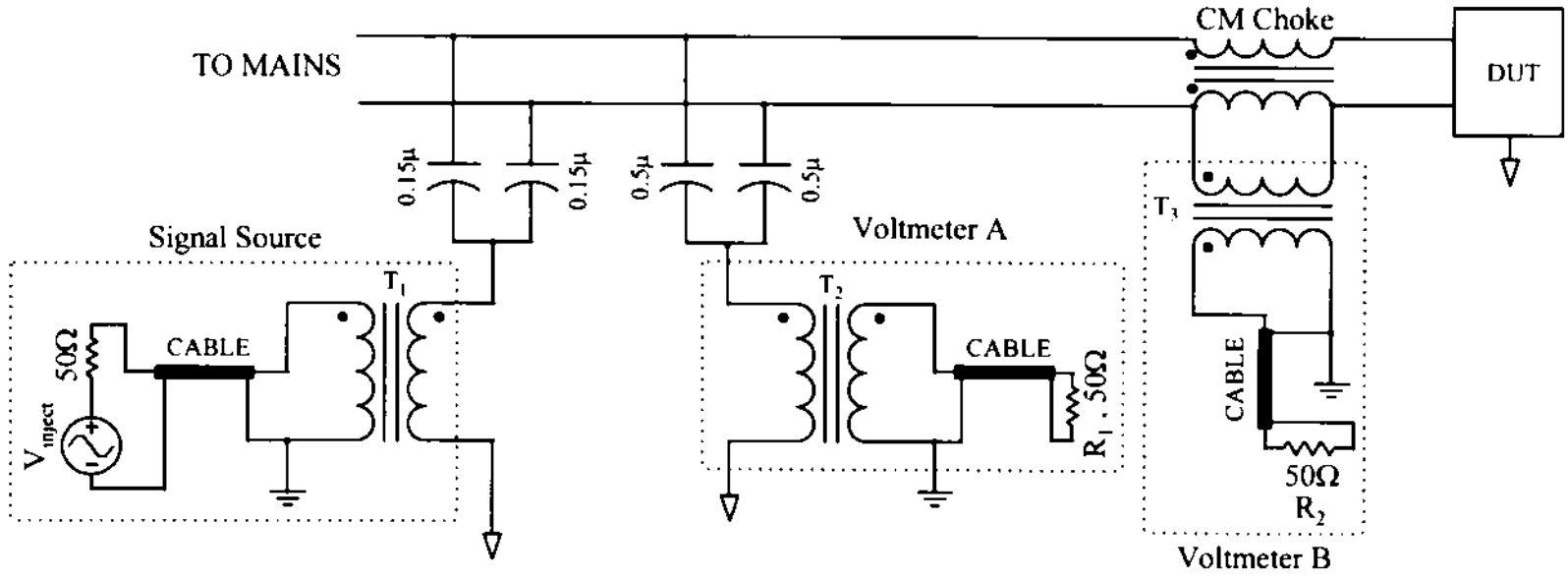

Fig. 3-13 Z_{scm} Measurement Setup

3.3 Special Issues Related to Off-line Power Supplies

The measurement of the source impedance of an off-line power supply is different from that of a dc/dc power supply in that the former has a rectifier which complicates the issue. For both CM and DM, there are two emission states that alternate with 120Hz cycle due to the "on" and "off" of the rectifier. That is, the CM and the DM source impedance are time-varying. The two emission states result in two impedance values for both DM and CM source impedance. However, for both CM and DM, it will be concluded that attention should be paid only to the impedance when rectifier is on. There will be a discussion about the correct measurement of DM source impedance during rectifier ON time. Again the rectifier plays an important role in this issue.

The arrangement of the following sections are as follows. First, two terms related to the off-line converter emission are defined so that the later discussions of the issues become easier. The measurement of CM source impedance is then considered. Then the more complicated DM source impedance measurement is explained. A measurement problem concerning the correct measurement of DM source impedance during diode bridge ON is discussed last.

3.3.1 Emission of Off-line Power Supplies

As discussed in Chapter II, due to the modulation of the diode bridge, the emissions are different depending on the state of the diode bridge. To better describe the phenomenon, please refer to Fig. 3-14. This figure shows the emission using the zero-

span mode of the spectrum analyzer. The zero-span mode enables the observation of the time-varying nature of the emission. This figure shows the zero-span at the fundamental switching frequency. The abscissa is time. It is clear in the figure that the fundamental frequency is amplitude modulated at 120Hz. For a detailed description of a spectrum analyzer's zero-span mode, refer to Section 2.4 on page 13.

ON PORTION - a section of the zero-span trace of a harmonic that coincides in time with the diode bridge ON state.

In Fig. 3-15, the marked time interval "*a*" corresponds to diode bridge ON state and therefore corresponds to an *ON PORTION*. There are altogether four *ON PORTIONS* in each trace in this figure, each *ON PORTION* occupying approximately 1.4ms, i.e. 17% of a 120Hz period.

OFF PORTION - a section of the zero-span trace of a harmonic that coincides in time with the diode bridge OFF state.

In Fig. 3-15, the marked time interval "*b*" corresponds to diode bridge OFF state and therefore corresponds to an *OFF PORTION*. There are three complete *OFF PORTIONS* in each trace of the figure.

Since the abscissa of a zero-span is time, all traces should be experiencing *their ON PORTIONs* simultaneously.

3.3.2 Measurement of Common Mode Source Impedance

As indicated in Section 3.1.1, source impedance can be calculated by using Eq.(10),

where |A| stands for the attenuation caused by the inserted series impedance. However, |A| value depends on the state of the rectifier as described earlier. Fig. 3-15 shows a measurement result of CM emission. The upper trace is the CM emission before and the lower trace is the CM emission after the insertion of a series impedance, and the difference in between is |A|. It can be seen that |A| is larger during the *ON PORTION* (*a* portion) than during the *OFF PORTION* (*b* portion). So in theory, there are two CM source impedances associated with CM emission, i.e. Z_{scm} (on) and Z_{scm} (off). However, the Z_{scm} (off) is not of practical importance for the reason explained below.

Fig. 3-16 shows the model of CM emission of the power supply. When the diode bridge is off, the whole CM loop impedance is higher, resulting in lower voltage at the load (LISN). Compared to diode bridge ON state, the diode bridge in OFF state acts like a series filter that attenuates the CM emission. No matter what type of filter is used, the attenuated CM during diode bridge OFF state can not be greater than that during diode bridge ON state. So the emission during diode bridge ON is the worst case. In other words, the standard measurement of CM noise measures the maximum of the trace which occurs at *ON PORTIONs*. Therefore, Z_{scm} (off) is of no practical significance.

Since the maximum value of the modulated CM emission is important, an efficient way to measure the CM attenuation is to use normal spectrum analyzer mode (instead of the zero-span mode) and activate the maximum hold function so that attenuations of

multiple harmonics can be measured simultaneously. Fig. 3-17 shows the result of such a measurement.

It may cause some doubt as to why *ON PORTION* is much larger than *OFF PORTION* for the upper trace in Fig. 3-15 whereas the two are almost the same in the lower trace. This can be explained as follows. When no series impedance is inserted, whether the diode bridge is on or it is off contributes significantly to the whole CM loop impedance. However, when the series impedance (a CM choke of large impedance) is in place, the loop impedance is much less dominated by the diode bridge and therefore the on or off of the diode bridge makes little difference to the CM emission. The conclusion is that the source impedance when the rectifier is on gives us the useful information while the other Z_{scm} (off) is of no practical use and should not be measured.

Conclusion:

Measure only the *ON PORTION* CM source impedance.

3.3.3 Measurement of DM Source Impedance

Similar to the CM emission, the DM emission varies according to rectifier state, as shown by the middle trace in Fig. 3-14. However, the issue is much more complicated for the DM situation. From the waveform, the *OFF PORTION* DM emission is higher than otherwise. In normal EMI emission measurement, one would have measured the peak of the emission which occurs at rectifier OFF state. However, if an X capacitor is used (bottom trace), the *OFF PORTION* emission is dramatically reduced while the

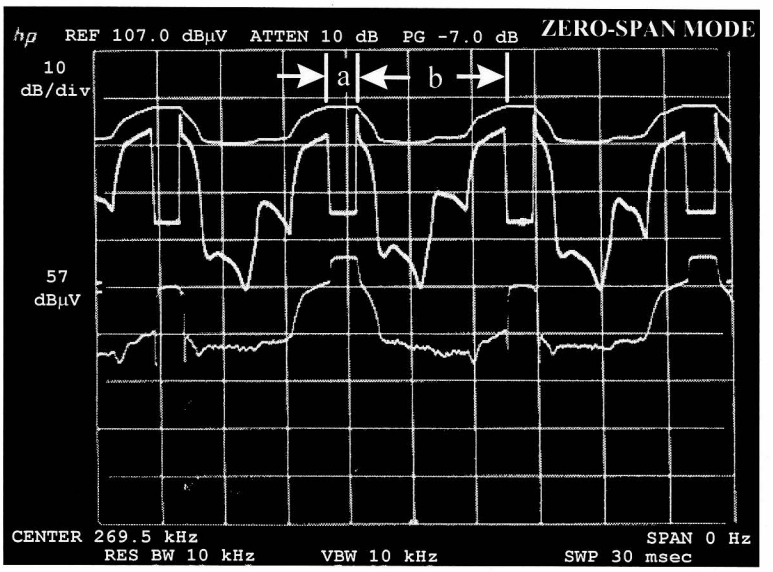

Fig. 3-14 Zero-Span (@269.5KHz) of Off-line Converter Emissions
Highest Trace: Baseline CM Emission
Middle Trace: Baseline DM Emission
Lowest Trace: DM Attenuated by An X Impedance (1μF~1Ω)

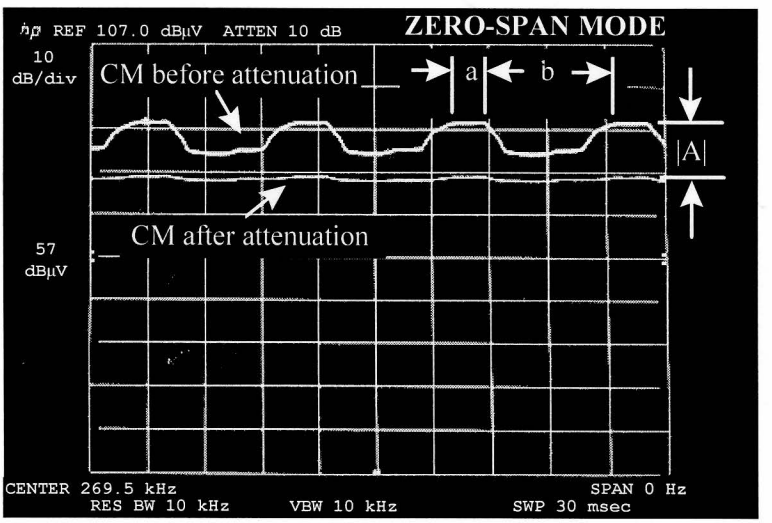

Fig. 3-15 CM Emissions (@269.5KHz) Before and
After the Insertion of A CM Choke

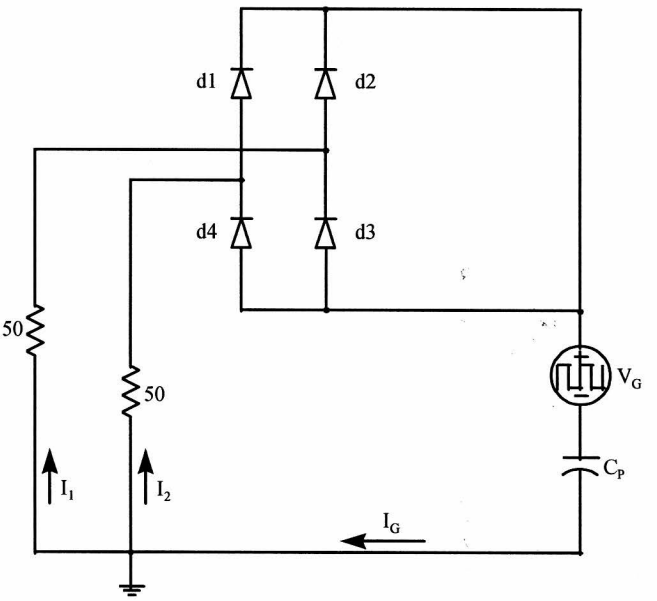

Fig. 3-16 CM Emission Pattern

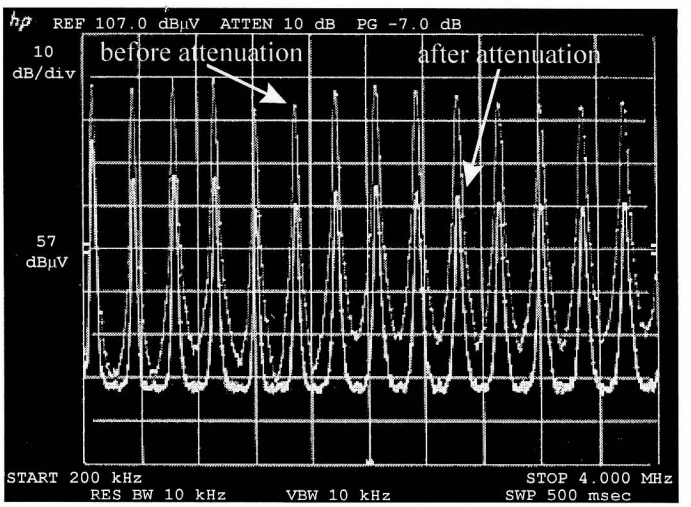

Fig. 3-17 CM Emissions Before and After Insertion of CM choke (*ON PORTIONS*), Frequency Range: 200KHz to 4MHz.

ON PORTION is reduced only a little, resulting in the peak emission occurring at ON state. This phenomenon is of importance and will be explained in the following two sections.

Effect of Circuit Unbalance During OFF PORTION

The DM emissions in an off-line converter may be dominated by the CM noise source when the circuit is unbalanced. This makes the measurement of DM source impedance more complicated than its CM counterpart. The following paragraphs explain the phenomenon in detail.

In Fig. 3-18, the upper trace shows the unfiltered DM emission. Obviously the *OFF PORTION* is much higher than the *ON PORTION* (as much as 20dB). The reason that *OFF PORTION* is huge can be explained by the model shown in Fig. 3-19. In Fig. 3-19 the diode pair d1-d3 are assumed to be the pair that is just turned off by the 60Hz current. However, due to the existence of the common mode noise source V_G (due to high frequency switching of the semiconductor switches in a power supply), d1 and d3 will conduct alternately depending on the polarity of V_G. Under the extreme situation, suppose d1 is an ideal open and d3 an ideal short, the DM generated by V_G is $I_{DM} = (I_2 - I_1) / 2 = (I_2 + I_1) / 2 = I_{CM} = I_G / 2$, i.e. V_G is generating CM and DM equally. So the CM source V_G is generating not only CM noise but also significant DM noise due to the extreme unbalance in the two legs (line and neutral) caused by the diode pair. Since the *OFF PORTION* is dominated by the common-mode-induced DM

(instead of the intrinsic DM), the elimination of it can be effectively achieved by balancing the two legs, as explained below.

Effect of Balancing the Circuit by an X Capacitor

The lower trace in Fig. 3-18 shows the dramatically attenuated *OFF PORTION* when an X capacitor is applied to balance the two legs. After the circuit is balanced, the *ON PORTION* stands out. The *ON PORTION* is considered to be dominated by intrinsic DM because both diodes conduct and the unbalance in the two legs is negligible.

OFF PORTION DM Source Impedance is of Little Importance

As explained above, the huge DM *OFF PORTION* is caused by extreme unbalance in the circuit and can be easily eliminated by balancing the circuit through the use of an X capacitor. Since most EMI filters contain at least one X capacitor, the circuit will be balanced automatically when the filter is applied. So when measuring the DM noise source impedance, the *OFF PORTION* should be ignored.

Unlike in the CM situation, zero-span mode has to be used to measure every harmonic since *ON PORTION* is non-distinguishable from the *OFF PORTION* in the normal spectrum analyzer mode.

Explanation of Two Other Phenomena in Emission Measurement

- *Broadband Noise*

Another phenomenon that happens at the beginning of the *OFF PORTION* is the broadband noise (see Section 2.3 for a detailed description). This is indicated by the 'spike' in Fig. 3-18. The broadband noise in an off-line power supply is caused by the turning off of the diode bridge. The current in the LISN inductors can no longer flow through the diode bridge and turn to flow through the spectrum analyzer causing a spike. It should be pointed out that similar to *OFF PORTION* emission, the broadband noise can also be easily eliminated by adding an X capacitor.

In Fig. 3-18 it can be noticed that any two adjacent *ON PORTION*s are different, especially for the lower trace. This brings a measurement problem because the attenuation to the *ON PORTION* by an X capacitor is not consistent. The conclusion is this problem can be eliminated by attenuating the CM first. The detailed explanation is as follows.

- *Inconsistent ON PORTIONs of DM Emission*

Notice the lowest trace in Fig. 3-14. There is an approximately 7dB difference between two adjacent *ON PORTIONS*. This makes measurement of the *ON PORTION* DM source impedance difficult. After some investigations, the reason was found. See Fig. 3-14 and Fig. 3-20. Since for adjacent *ON PORTIONS*, different diode pairs conduct, DM currents at the LISNs are 180° out of phase, just like the two vectors *B* and *C*. However, CM currents for adjacent *ON PORTIONS* are in phase, as indicated by

the vector A. The DM detector (180° power combiner) at the LISNs RF ports has a limited common mode rejection ratio (CMRR), typically 40dB. Therefore what we observe at the output end of the DM detector is the (vector) sum of CM residual and DM. Since the CM in Fig. 3-14 is huge, even after being attenuated by 40dB, the residual is still not too smaller than the DM, as indicated by the vector D. So for the first *ON PORTION*, $|B+D|$ appears at the output of the DM detector, whereas for the second *ON PORTION*, $|C+D|$ which equals $|-B+D|$ appears at the output of the DM detector.

The explanation was further verified by significantly reducing the CM current at the LISNs. Fig. 3-21 shows a similar set of traces as Fig. 3-14 except that an LC CM filter was applied. Apparently the *ON PORTIONS* of the lowest trace are equal now.

So it is always desirable to seek a DM detector with as much CMRR as possible. It is also common practice to attenuate one mode before measuring the other mode.

In the present case, it is generally not correct to take the arithmetic mean of two adjacent *ON PORTIONS* to obtain the true DM because CM and DM are adding in vector space instead of scalar space.

3.4 Finding The Source Impedance Of An Off-Line Converter By ILM

The source impedance of an off-line converter is to be measured using the two proposed methods. First the measurement of attenuation is described. Then the source impedance is calculated. Finally the source impedance is verified.

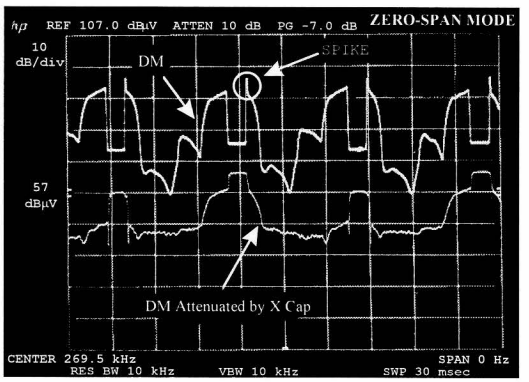

Fig. 3-18 DM Emission Before and After the Insertion of an X Capacitor (See the "X Cap" in Fig. 3-19)

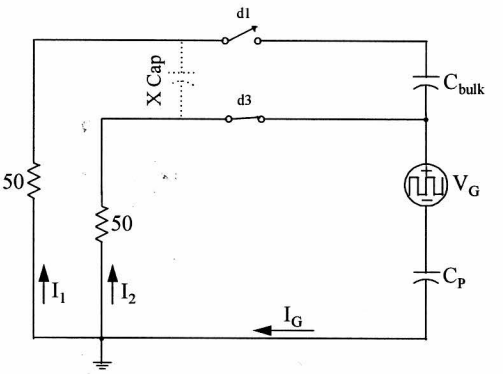

Fig. 3-19 Circuit Unbalance During Rectifier OFF Time (ignore X Cap)

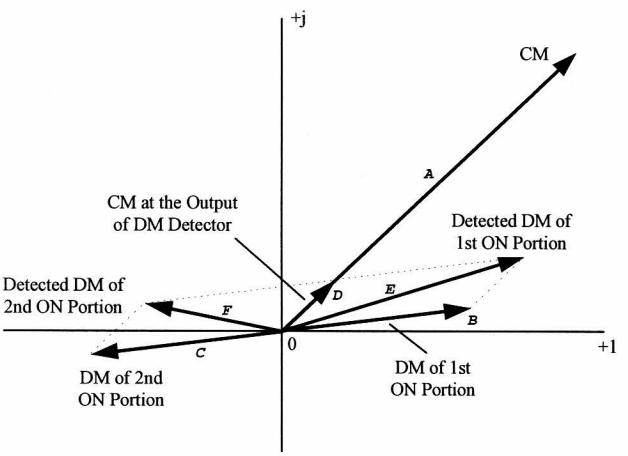

Fig. 3-20 Inconsistent *ON PORTIONs* of DM Emission

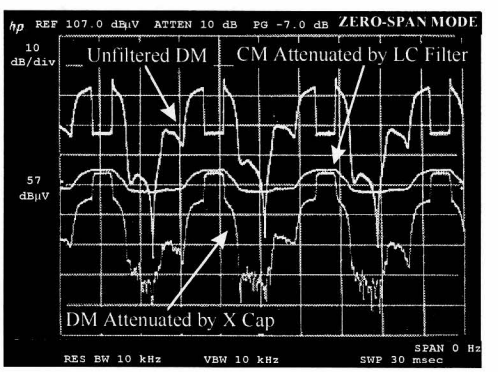

Fig. 3-21 Zero-Span of Fundamental CM and DM Components when there is an LC CM filter (refer to Fig. 3-28 for setup)

3.4.1 *Description of DUT and Equipment Needed*

The power stage of the converter was shown in Fig. 2-5 and is to be repeated here as Fig. 3-22. A photograph of the whole converter (not including the other half of the chassis) is shown in Fig. 3-23.

Specifications of the DUT:

V_{in} = 120VAC, V_{out} = 15VDC, P_{omax} = 60W, f_s = 269.5KHz @ 3.5Watts, Fully Enclosed in a Metal Chassis, EMI Filter Removed.

The equipment needed is: two single-line LISNs, a 0° and a 180° power combiner, a spectrum analyzer and a screen room. A photo of the test site is shown in Fig. 3-24.

3.4.2 *Measurement of Attenuation and Filter Impedance*

Common Mode

Since the CM source impedance is usually very large ($>>25\Omega$), the series insertion method is used. The measurement setup is shown in Fig. 3-25. The spectra of CM emissions before and after a CM choke was applied are shown in Fig. 3-17 and are repeated in Fig. 3-26. To calculate CM source impedance, the attenuation $|A|$ and choke impedance $|Z_{series}|$ are needed. The attenuation is obtained by finding the difference between corresponding harmonics of the two measurements. For example, at the fundamental frequency (269.5KHz), the baseline CM emission is 95dBμV and the attenuated CM is 81.9dBμV. Therefore the attenuation is: 95dBμV - 81.9dBμV = 13.1dB. The CM choke impedance $|Z_{series}|$ can be found by an impedance analyzer.

In Fig. 3-25 , the two 100KΩ damping resistors are used to control the impedance of the CM coil near its self-resonant frequency otherwise the coil impedance would both be too large and sensitive to ambient structure such as a piece of metal nearby.

The corresponding measurement results are listed in Table I below and also shown graphically in Fig. 3-27.

Table I. CM Source Impedance Measurement Data

Frequency (MHz)	0.27	0.54	0.82	1.1	1.37	1.65	1.92	2.2	2.47	2.75	3.02	3.3	3.58	3.85
$\lvert Z_{sens}\rvert$* (KΩ)	31	39	32	26	22	19	16	14	13	11.4	10.4	9.6	8.8	8.2
Attenuation (dB)	13.1	21.1	22.3	23	23.4	23.3	23.5	23.6	23.6	23.6	23.3	23.5	23.7	23.6

**CM Choke Data: Core = TDK H5B-T14.5-20-7, μ_i = 5000, Turns Per Winding = 87, Winding Technique = Bifilar, Parallel Damping Resistor Per Winding = 100KΩ*

Differential Mode

It has been mentioned in Section 3.3 that in the case of an off-line converter, the diode bridge may cause measurement difficulties such as inconsistent DM attenuation, due to the limited CMRR of the DM detector. One way to overcome this problem is to attenuate the CM emission first so that the CM residual appearing at the output of the DM detector is well below the DM level. See Fig. 3-28 for measurement setup.

In the setup, the DUT is floating, and C_g represents the chassis-to-ground capacitance. Since C_g is usually very small (tens of pico-farads), the chassis-to-ground impedance is therefore very large (higher than that of the most effective CM choke). The two Y capacitors (C_{Y1} and C_{Y2}) and C_g form a very effective second order CM filter. This filter completely eliminates the CM residual problem discussed in Section 3.3.3.

Since the DM source impedance during *ON PORTION* is found to be of low impedance (by trial and error), the shunt insertion method is applied. The shunt component is the series combination of a 1Ω resistor and a 1μF capacitor. The 1Ω resistor is used to dominate the shunt impedance so that the difficult-to-account-for self resonance of the 1μF capacitor will not become a significant source of error.

As an illustration, Fig. 3-29 shows the zero-span at the fundamental frequency (269.5KHz) of DM emission before and after the insertion of the shunt component. The *ON PORTION* before attenuation is 71.7dBμV, and that after attenuation is 58.9dBμV. So the attenuation at the fundamental frequency is: 71.7dBμV - 58.9dBμV = 12.8dB.

The attenuation and impedance of the shunt component up to near 4MHz are listed in Table II and also shown graphically in Fig. 3-30.

Table II. DM Source Impedance Measurement Data

Frequency (MHz)	0.27	0.54	0.82	1.1	1.37	1.65	1.92	2.2	2.47	2.75	3.02	3.3	3.58	3.85
$\lvert Z_{shunt} \rvert$ * (Ω)	1.18	1.06	1.04	1.03	1.04	1.04	1.05	1.06	1.07	1.08	1.09	1.1	1.12	1.13
Attenuation (dB)	12.8	13.2	13.3	13.5	13.4	13.4	13.7	13.7	13.9	14.1	14.1	14.3	14.6	14.9

3.4.3 Calculation of Source Impedance

With the information of measurement filter impedance and filter attenuation, noise source impedance can be readily found simply by applying the two formulas Eqs.(10) and (13) developed in Section 3.1 (*see* Page 19). For easy reference, the two equations are shown below.

$$|Z_s| \approx \frac{|Z_{series}|}{\sqrt{||A|^2 - 1|}} \qquad (10)$$

$$|Z_s| \approx |Z_{shunt}| \times \sqrt{||A|^2 - 1|}, \qquad (13)$$

Common Mode

As an illustration, the calculation of CM source impedance at the fundamental frequency will be shown in detail. From Table I, it is known that at the fundamental frequency (269.5KHz), $|Z_{series}|$ = 31KW, and $|A|$ = 13.1dB = 4.52 (times). By applying Eq.(10), the CM source impedance is:

$$|Z_{scm}| \approx \frac{|Z_{series}|}{\sqrt{||A|^2 - 1|}} = \frac{31K\Omega}{\sqrt{|4.52|^2 - 1}} = 7.0K\Omega. \qquad (16)$$

CM source impedance at other frequencies can be calculated in the same manner. The result is listed in Table III and also shown graphically in Fig. 3-31.

Table III. CM Source Impedance and Measurement Data

Frequency (MHz)	0.27	0.54	0.82	1.1	1.37	1.65	1.92	2.2	2.47	2.75	3.02	3.3	3.58	3.85
$\|Z_{series}\|$ (KΩ)	31	39	32	26	22	19	16	14	13	11.4	10.4	9.6	8.8	8.2
Attenuation (dB)	13.1	21.1	22.3	23	23.4	23.3	23.5	23.6	23.6	23.6	23.3	23.5	23.7	23.6
$\|Z_{scm}\|$ (Ω)	7030	3449	2463	1845	1491	1302	1072	927	861	755	713	643	576	543

From the Bode plot of the magnitude of Z_{scm}, it is apparent that the CM source impedance is very close to purely capacitive. It would be therefore unnecessary to use the Hilbert transform to derive phase.

Differential Mode

Because a shunt component is used to derive the DM source impedance, Eq.(13) should be used. The shunt impedance at the fundamental frequency is $|Z_{shunt}| = 1.18\Omega$, and the attenuation is $|A| = 12.8\text{dB} = 4.37$ (times). So the DM source impedance at the fundamental frequency is:

$$|Z_{sdm}| \approx |Z_{shunt}| \cdot \sqrt{||A|^2 - 1|} = 1.18\Omega \times \sqrt{4.37^2 - 1} = 5.02\Omega. \qquad (17)$$

DM source impedance at other frequencies can be calculated in the same manner. The result is listed in Table IV and also shown graphically in Fig. 3-32.

Table IV. DM Source Impedance Measurement Data

Frequency (MHz)	0.27	0.54	0.82	1.1	1.37	1.65	1.92	2.2	2.47	2.75	3.02	3.3	3.58	3.85
$\|Z_{shunt}\|$ (Ω)	1.18	1.06	1.04	1.03	1.04	1.04	1.05	1.06	1.07	1.08	1.09	1.1	1.12	1.13
Attenuation (dB)	12.8	13.2	13.3	13.5	13.4	13.4	13.7	13.7	13.9	14.1	14.1	14.3	14.6	14.9
$\|Z_{sdm}\|$ (Ω)	5.01	4.73	4.69	4.76	4.75	4.75	4.97	5.02	5.19	5.37	5.42	5.60	5.91	6.18

3.4.4 Verification of Source Impedance

There are several ways to verify the measured source impedance. One way is to use a filter component with different value and compare the predicted and measured attenuation. A second way is to examine the internal structure of the DUT and determine the component that dominates the source impedance.

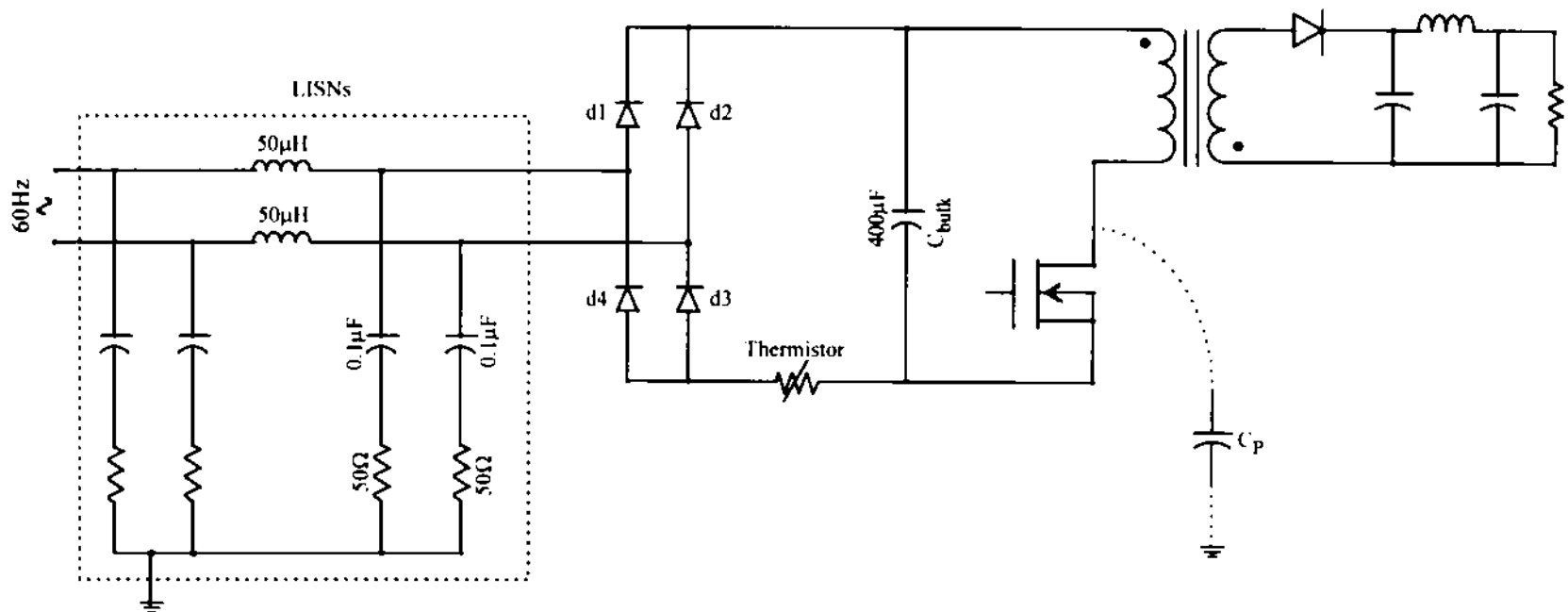

Fig. 3-22 Measuring Conducted Emissions of An Off-Line Flyback Converter

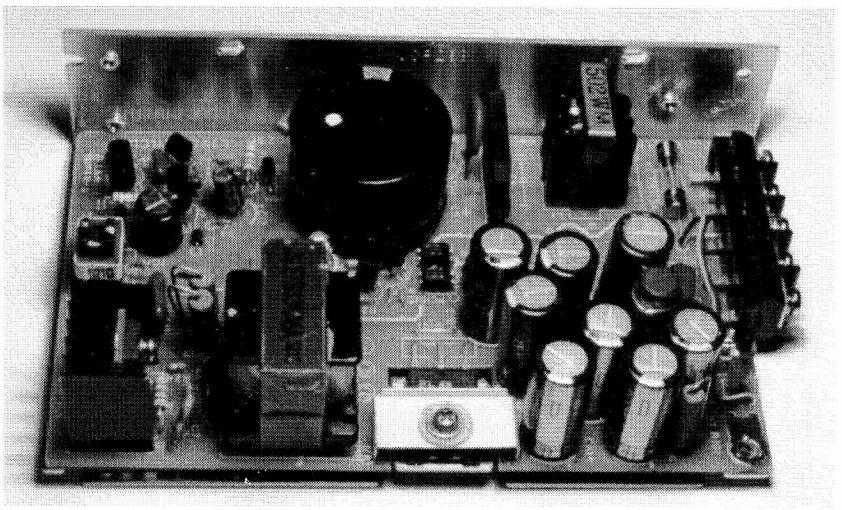

Fig. 3-23 A Photo of the DUT (Part of Chassis Removed)

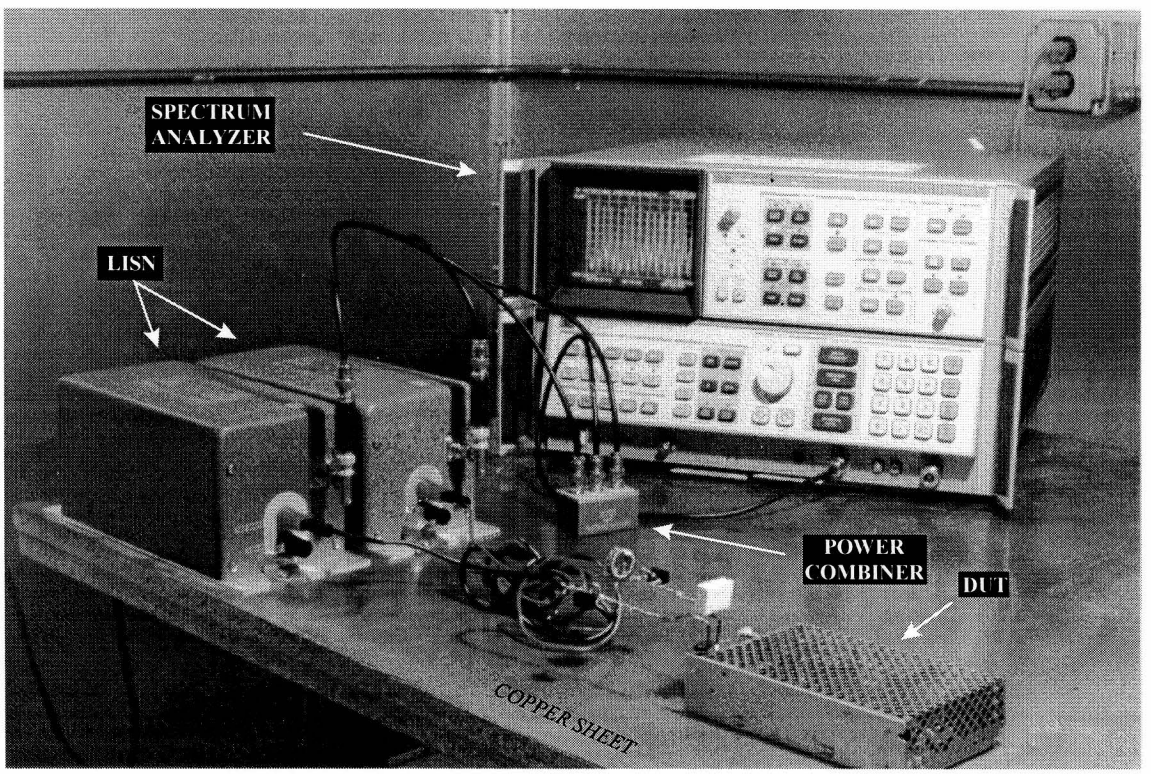

Fig. 3-24 A Photo of the Measurement Setup in An EMI Lab

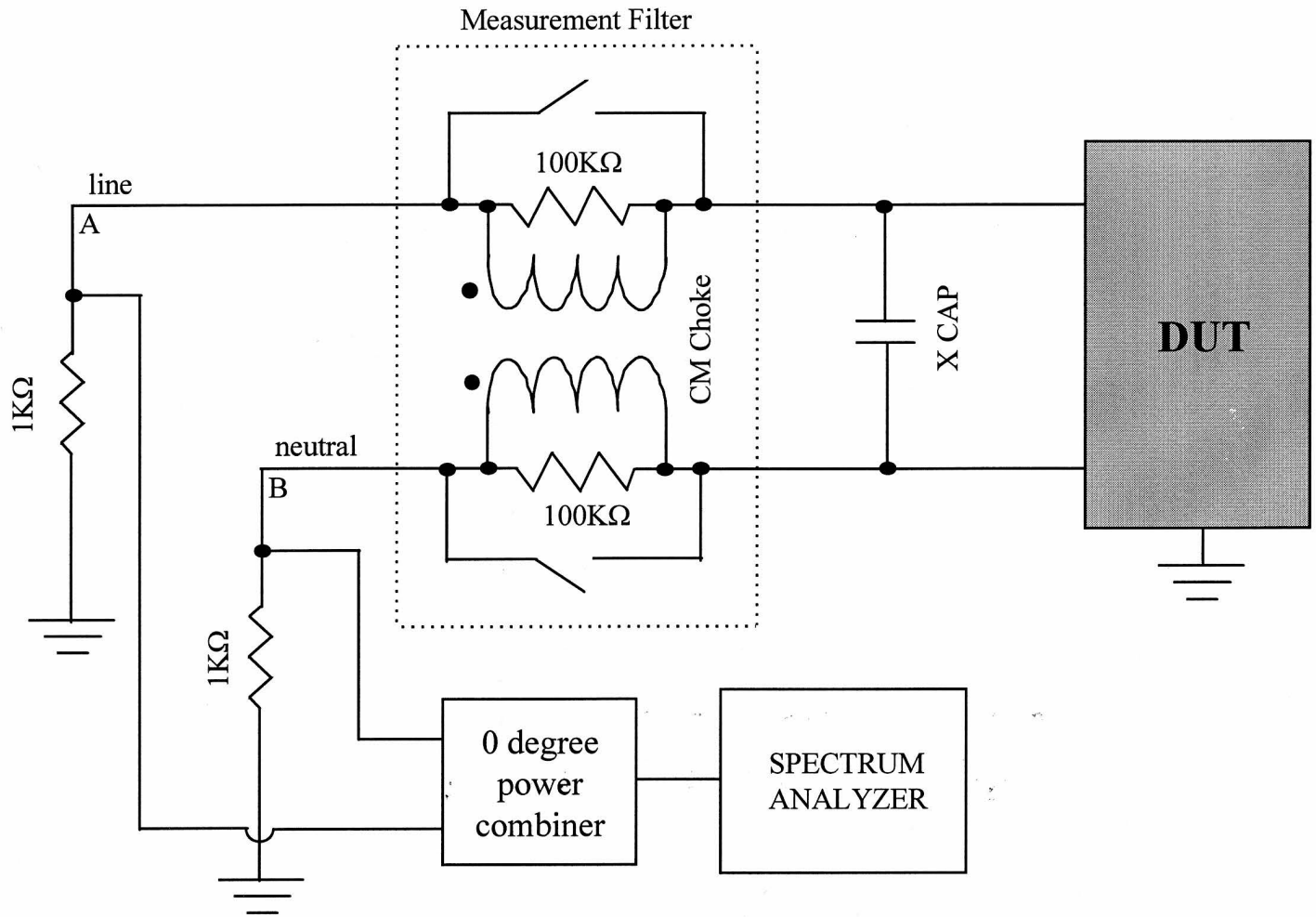

Fig. 3-25 Setup for Measurement of CM Source Impedance

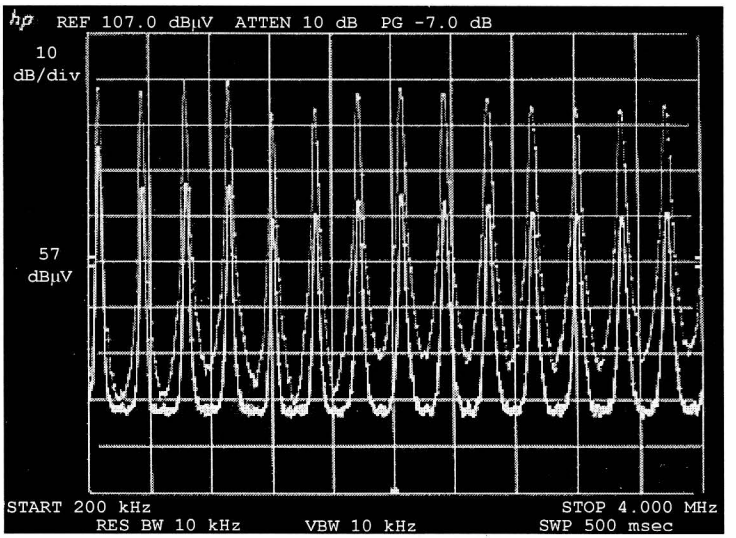

Fig. 3-26 CM Emissions Before and After Insertion of CM choke (*ON PORTIONS* only)

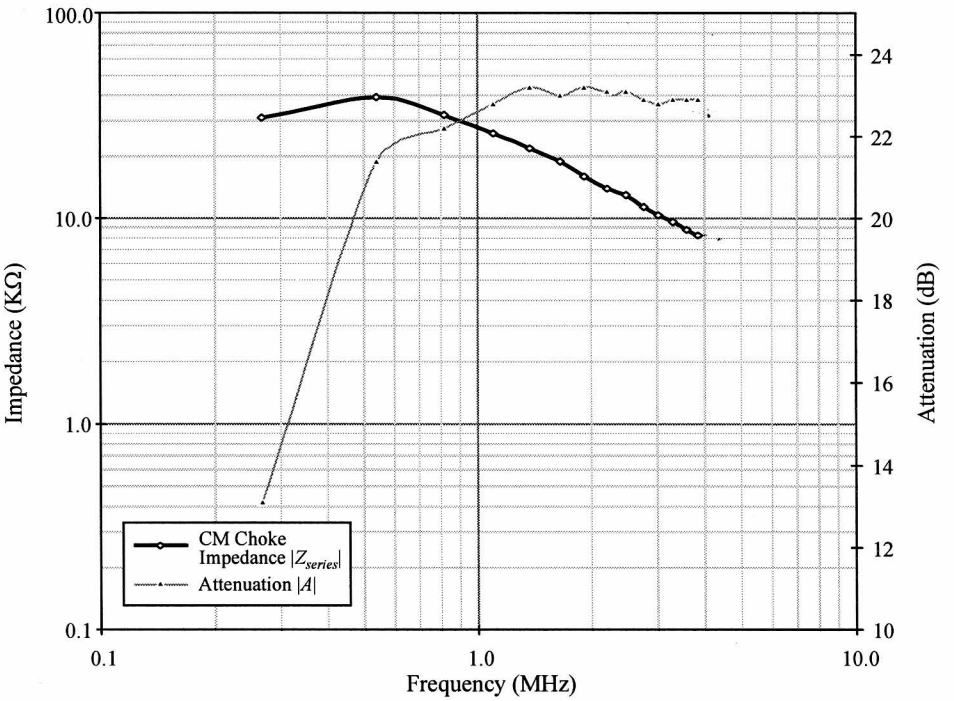

Fig. 3-27 CM Choke Impedance and Attenuation

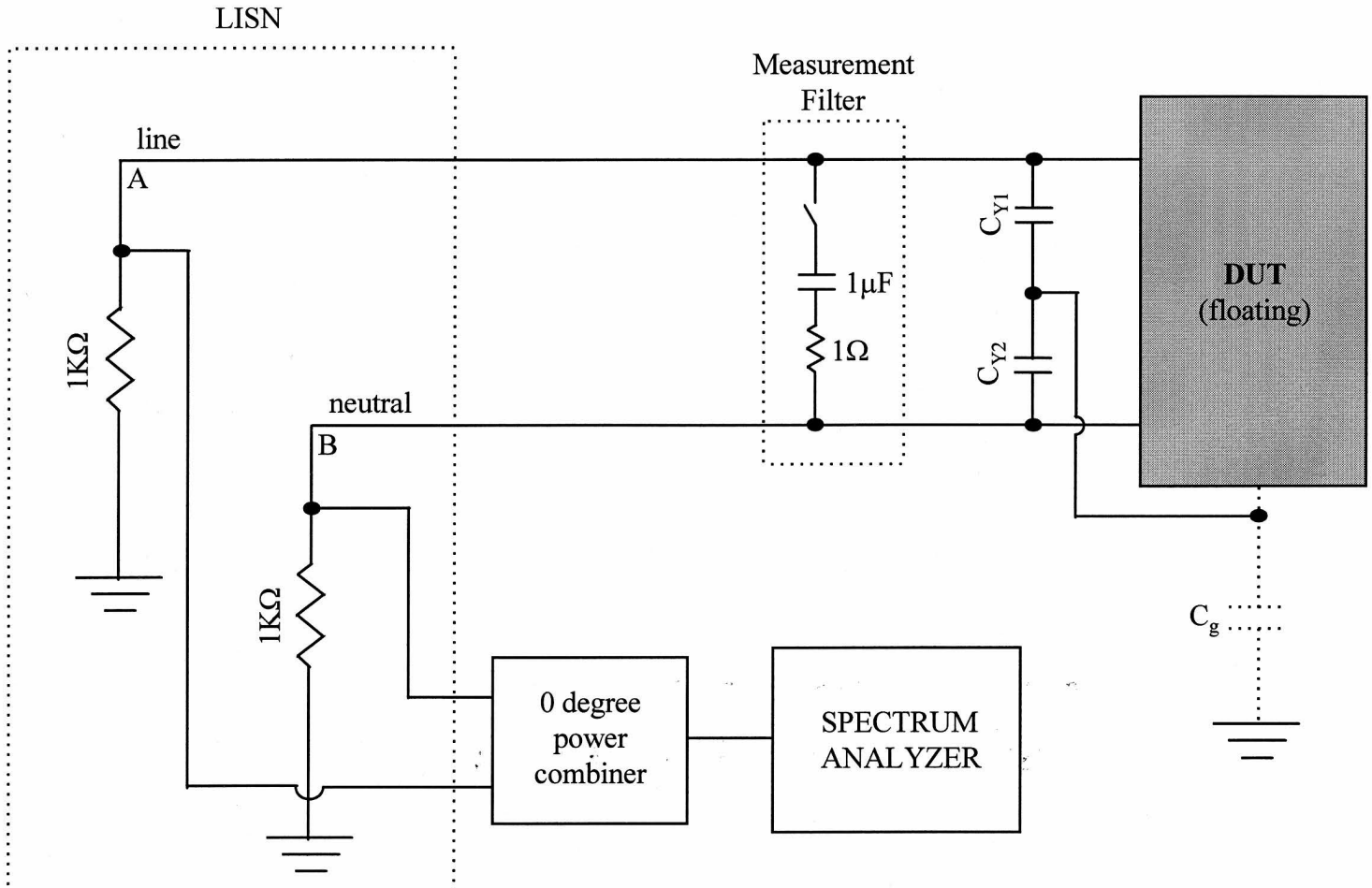

Fig. 3-28 Setup for Measurement of DM Source Impedance

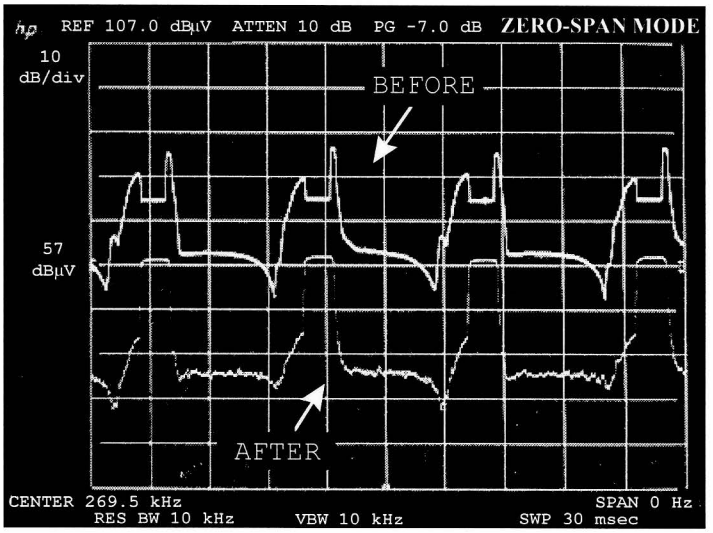

Fig. 3-29 Zero-Span of DM Emission at Fundamental Frequency (269.5KHz) Before and After Insertion of Shunt Component

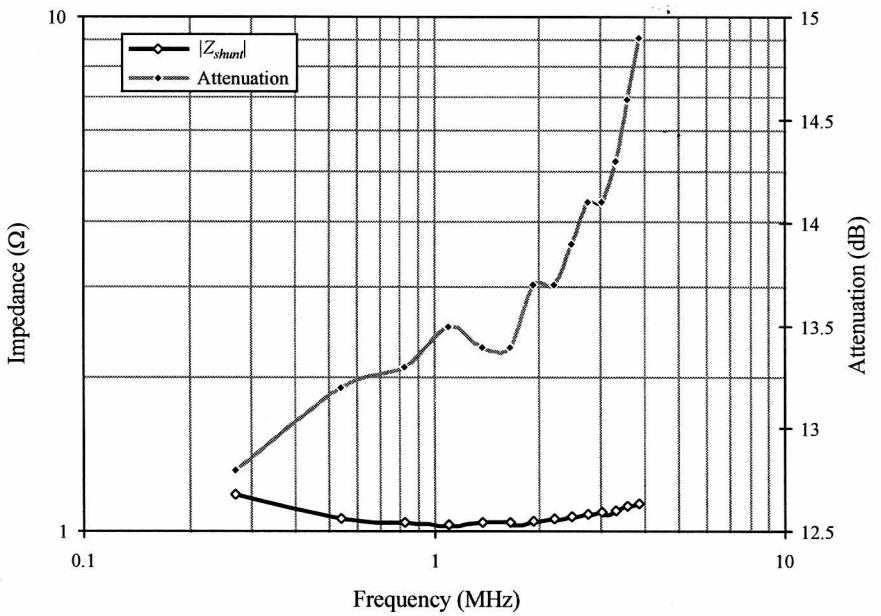

Fig. 3-30 Shunt Component Impedance and Attenuation

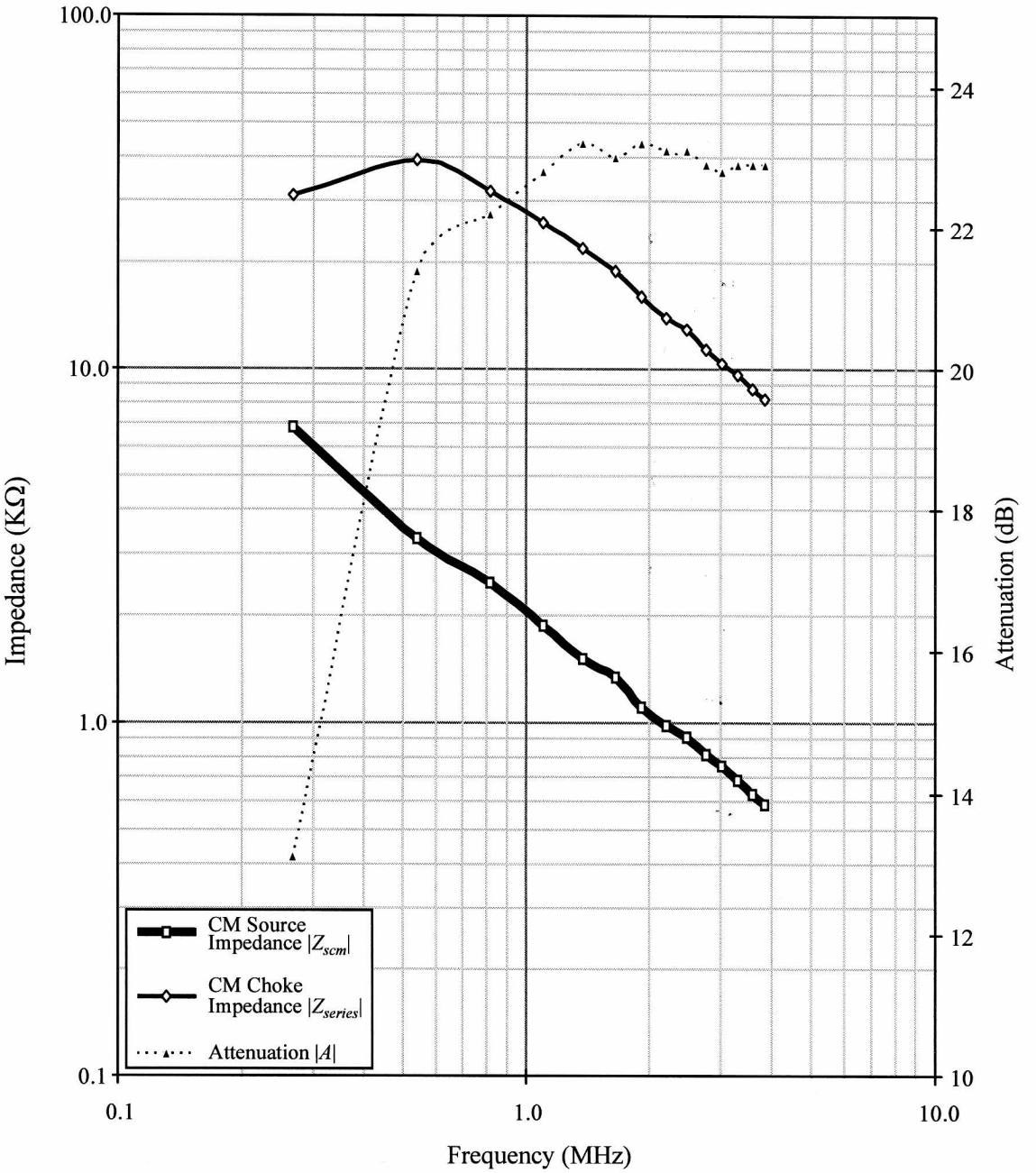

Fig. 3-31 CM Source Impedance, CM Choke Impedance and Attenuation

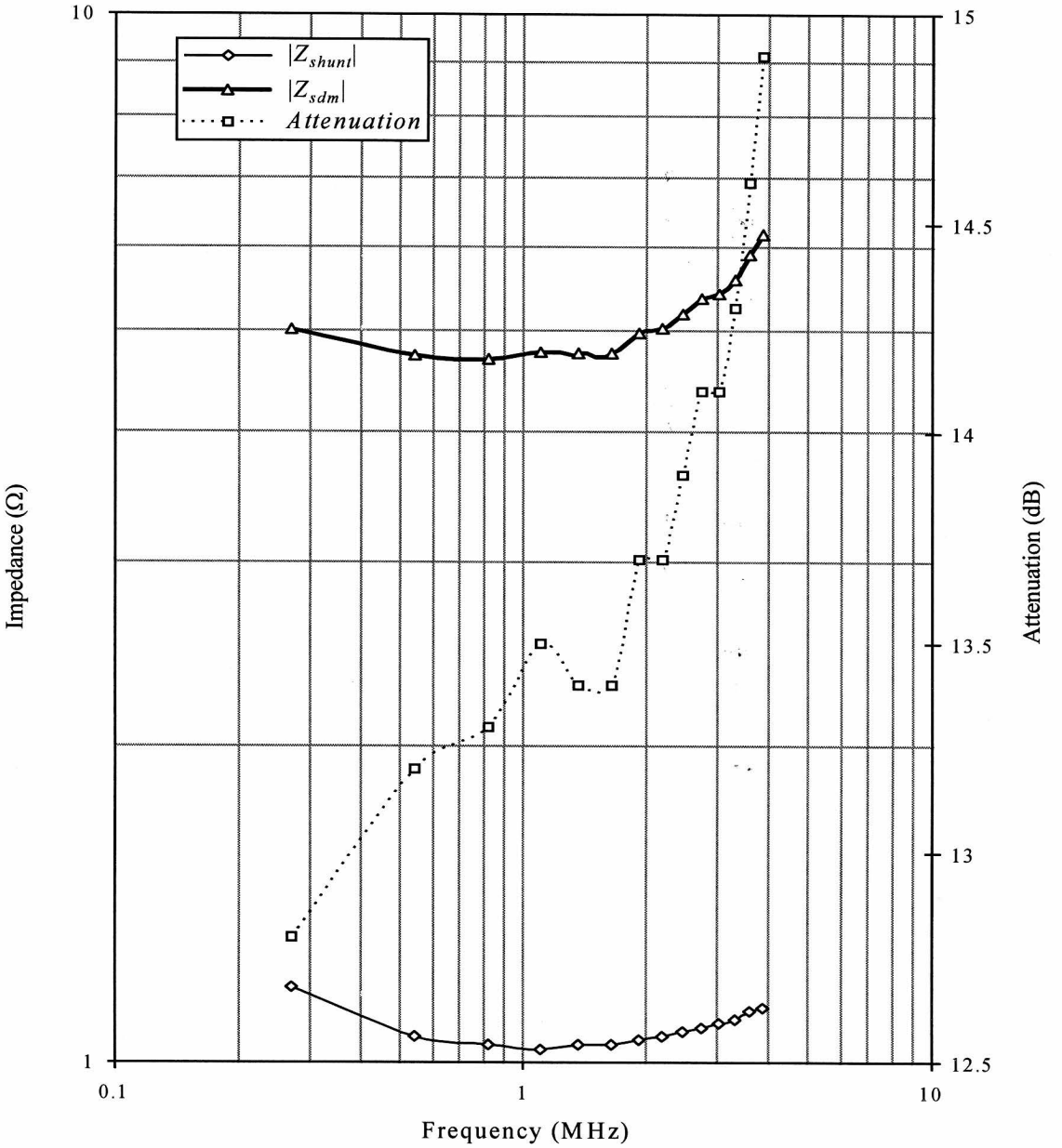

Fig. 3-32 DM Source Impedance, Shunt Component Impedance and Attenuation

Common Mode

The first way to verify the CM source impedance is to use a CM choke that has a different impedance than the original one, and see if the measured attenuation of the new choke agrees with the predicted. Fig. 3-33 shows the result of such a test. Clearly, the measured and predicted attenuations agree very well. The construction data for the new choke is listed below as a reference.

Core = TDK H5B-T14.5-20-7, μ_i = 5000, Turns Per Winding = 42, Winding Technique = Bifilar.

Another way to confirm the rough range of the CM source impedance is to insert an LC filter and compare the predicted and measured attenuation. As has been indicated, it only verifies the rough range of the source impedance, due to the nature of a second order filter.

Fig. 3-34 shows the measurement setup. The corresponding comparison result is shown in Fig. 3-35. It can be seen that the difference between the two is within 2dB.

Differential Mode

Since the measured DM source impedance is of very low value (several ohms), it is not very effective to verify it by using another shunt component because it is difficult to know exactly the impedance value of a shunt component if it is less than 1Ω. Thus instead of using the approach in the CM verification, the measured DM source impedance is directly verified by examining the structure of the DUT, see Fig. 3-36. Suppose diodes d1 and d3 are on, the impedance to the right of the bulk capacitor is virtually

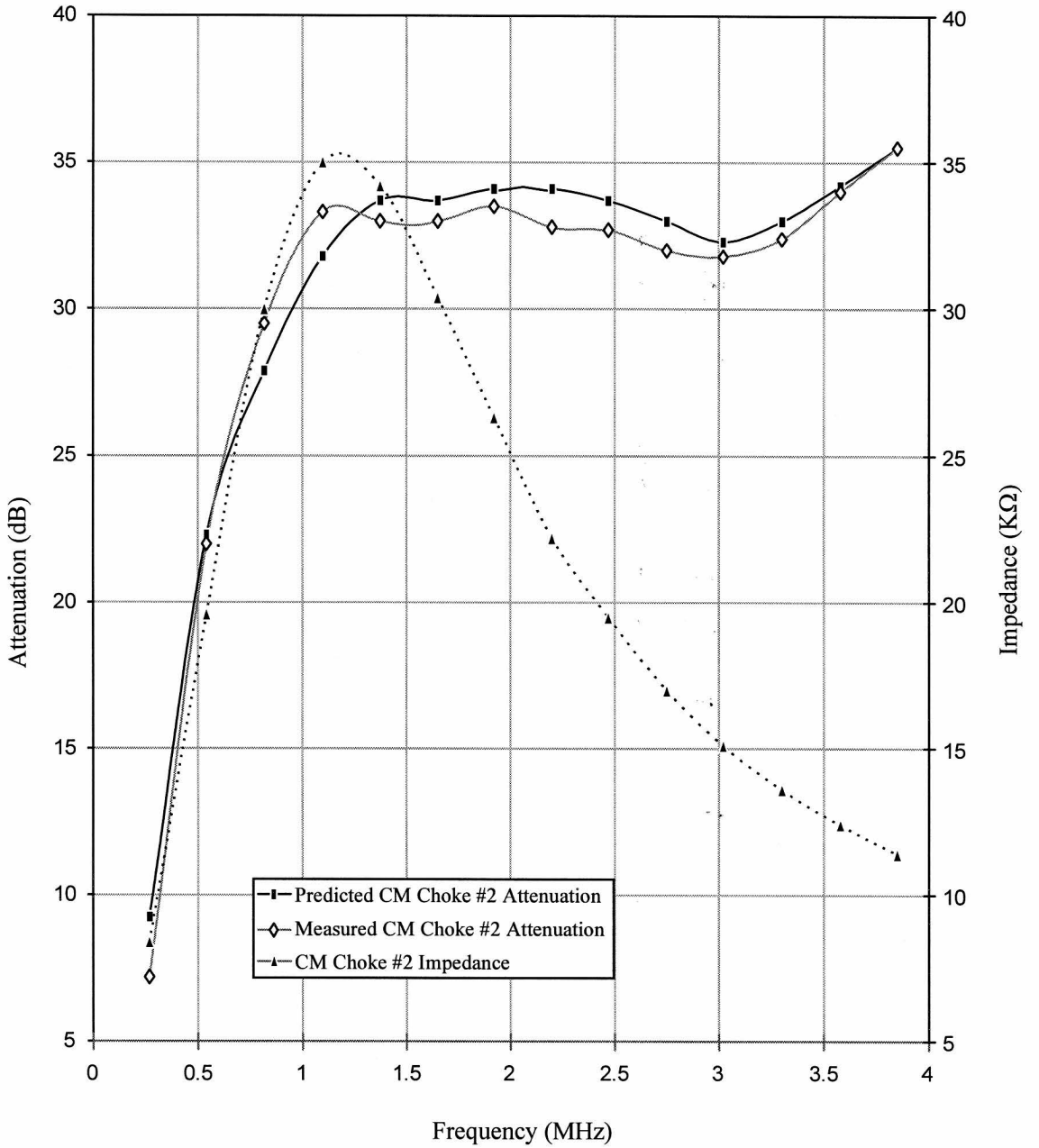

Fig. 3-33 Measured / Predicted CM Attenuations and the Impedance of a New CM Choke

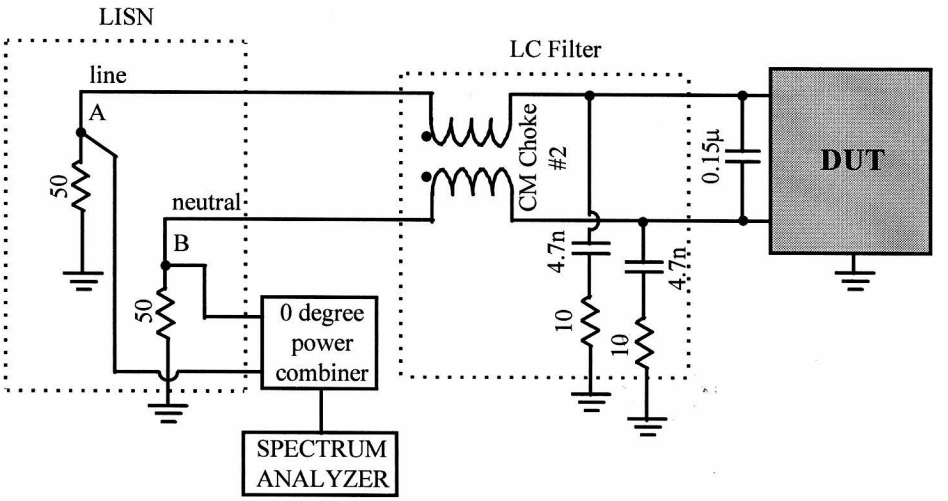

Fig. 3-34 Setup to Verify the Rough Range of the CM Source Impedance

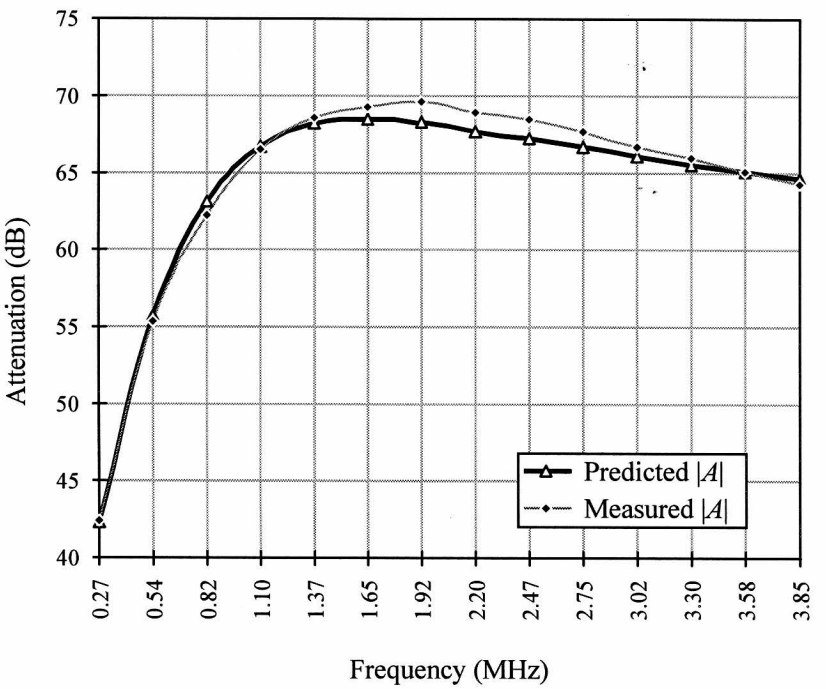

Fig. 3-35 Comparison Between Measured and Predicted CM Attenuations of an LC Filter

shorted by it. The thermistor is found to have a resistance of approximately 4.8Ω when the circuit is operating and therefore is the dominant impedance in the DM path when the diode bridge is on. This strongly agrees with the Table IV data. The fact that the measured DM source impedance goes up gradually with frequency suggests that the DM current loop inductance starts to come into picture when the frequency becomes higher.

3.5 Finding The Source Impedance Of An Off-Line Converter By SIM

The measurement setup is shown in Fig. 3-12 and Fig. 3-13. The measurement of source impedance by the Signal Injection Method is also complicated by the existence of a diode bridge in the DUT.

In the case of CM, little problem was encountered since the source impedance was dominated by the circuit-to-chassis capacitance so the state of the diode bridge did not have significant influence on measurement results. A plot of the measured CM source impedance is shown in Fig. 3-37. The spikes in the two curves are the result of DUT emission. For example, the callout saying "Fundamental" indicates that the spike was caused by the fundamental component of the DUT noise. From the figure it is apparent to tell that measured impedance is highly capacitive, and its value is close to the result obtained by Insertion Loss Method.

In the case of DM, the source impedance varies dramatically when the diode bridge changes state. If the measuring device has fast enough responding speed, it can be syn-

chronized with *ON PORTIONs*, and acquire data only during the diode bridge ON state, i.e., a gated measurement. However, the gain-phase analyzer is apparently not fast enough. This is evidenced by the displayed DM source impedance curve being highly wrapping: it swings very fast between several Ohms and several Kilo-ohms. Under such a situation, no guarantee can be made about the accuracy of the measurement result. Assume the instantaneous impedance curve is an accurate representation of what is happening in the DUT, then the *ON PORTION* DM source impedance can be found simply by picking the lower envelope of the recorded curve. Unfortunately, the original gain-phase analyzer plot of the measurement result was not preserved and thus cannot be listed here.

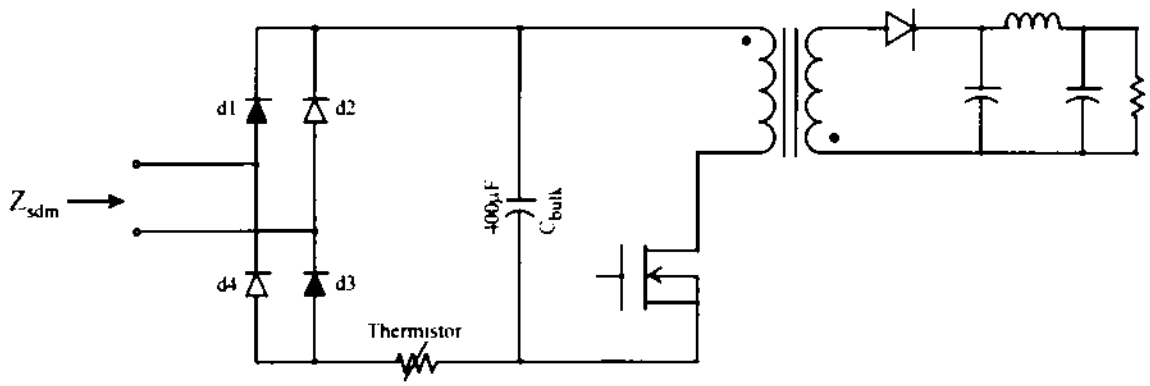

Fig. 3-36 Verify the DM Source Impedance From DUT Structure

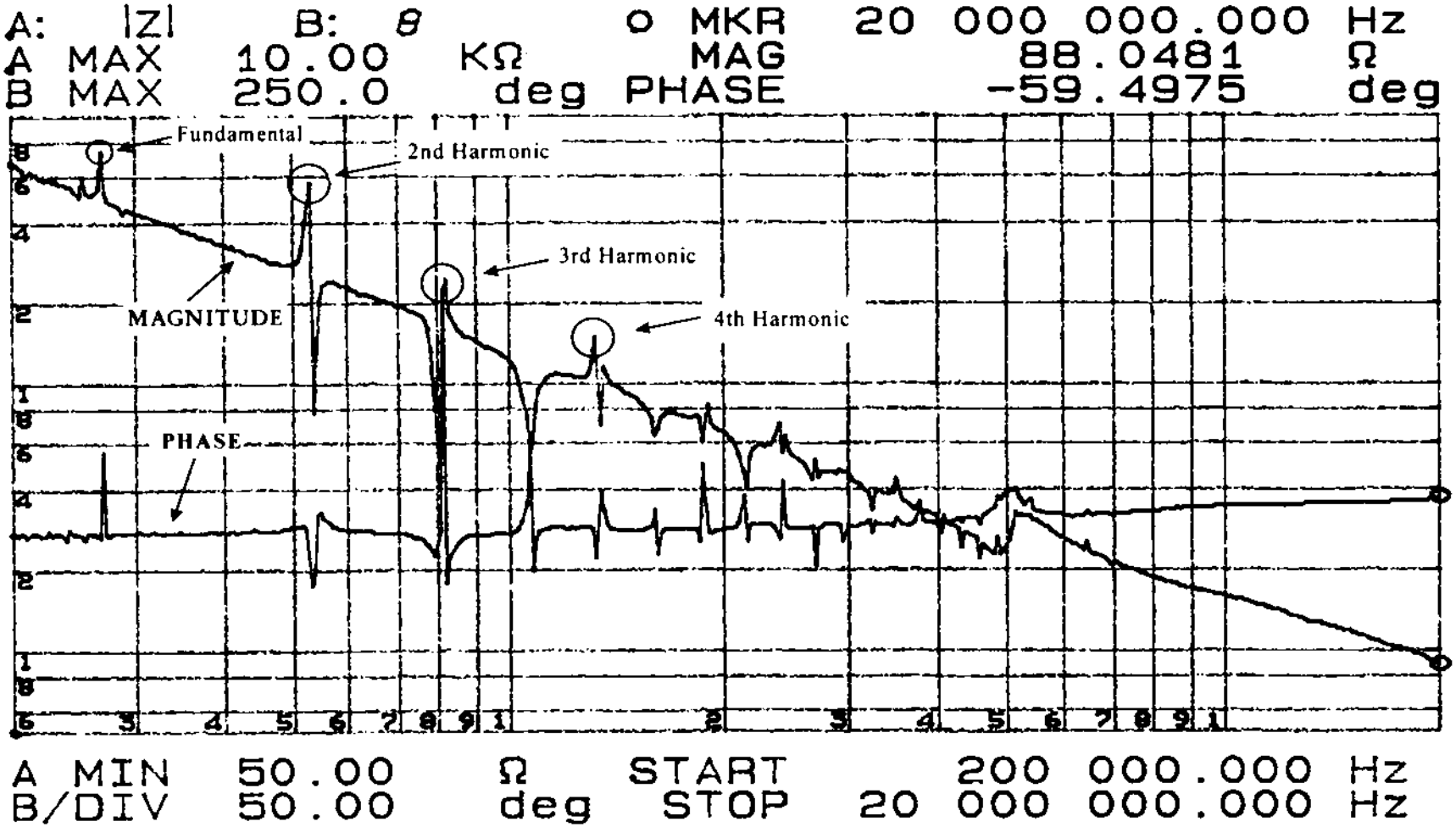

Fig. 3-37 CM Source Impedance by Signal Injection Method

Chapter IV
CHARACTERIZING EMI FILTERS BY THE [Z] MATRIX APPROACH

As mentioned in Chapter I, the performance of an EMI filter depends not only on the filter itself but also on the noise source impedance and the noise load impedance. Up to date, all commercially available EMI filters are characterized by filter attenuation curves published in the manufacturers' catalogs. These attenuation curves are obtained with a 50Ω system, i.e. both the source impedance and the load impedance are assumed 50Ω. In reality, the source and load impedance of a power supply can be very much different from 50Ω and therefore, the manufacturers' published attenuation curves could deviate significantly from reality. In the past, due to the lack of knowledge of noise source impedance, further effort to characterize these filters was not very meaningful. However, as a result of the studies discussed in Chapter III, source impedance information is no longer difficult to obtain. It then becomes a rewarding practice for EMI filter manufacturers to properly characterize their products since prediction of filter effectiveness becomes practical.

In this chapter, a new method to characterize EMI filters is proposed. Instead of characterizing the filter by attenuation curves as conventionally done, it is proposed that the filter be characterized by its impedance matrix. This can be done independ-

ently without having to assume source or load impedance. From the impedance matrix obtained, the filter attenuation curves can be calculated using a formula developed in this chapter. An impedance / gain-phase analyzer was used for such characterization and the results obtained were verified experimentally. This method automatically takes parasitic effects into consideration and is accurate even at very high frequencies (>10MHz).

4.1 Characterization Of A Linear Passive Two-Port Network

For the benefits of later discussion, two-port network theory will be reviewed in this section first [5].

For a linear passive two-port network, there are four external variables. Namely, Port #1 voltage V_1 and current I_1, Port #2 voltage V_2 and current I_2, as shown in Fig. 4-1. The relationship among these four variables can be used to fully describe the external behavior of the two-port network. Two linear equations are needed to describe the system. Each linear equation expresses a variable in terms of the linear combination of two other variables. Different combinations of these equations give us six different pairs of equations, whose coefficient matrices are commonly referred to as [Z], [Y], [G], [H], and [$ABCD$] etc. Selection of proper matrix to model the network depends on the application and the ease of parameter measurement. Some of the parameters are more difficult to measure than others when the frequency is high. For example, the A

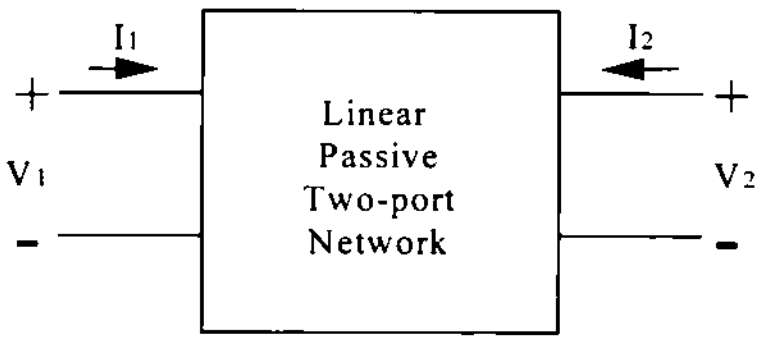

Fig. 4-1 Representation of a Linear Two-Port Network

parameter in the [*ABCD*] matrix (defined as V_1 / V_2 when $I_2 = 0$) requires the measurement of Port #2 open circuit voltage. This is difficult to achieve at high frequencies due to parasitic capacitance. Another example is the *B* parameter (defined as $-V_1/I_2$ when $V_2 = 0$) which requires the measurement of short circuit current. This is also difficult to achieve at high frequencies because of parasitic inductance.

The conclusion is that transfer functions are more difficult to measure than driving-point functions at high frequencies due to the necessity to measure open-circuit voltages or short-circuit currents. (A transfer function is defined as the ratio of two variables of different ports, while a driving point function is defined as the ratio of two variables of the same port. For example, V_2/I_1 is a transfer function whereas V_2/I_2 is a driving point function.)

An EMI Filter As A Two-Port Network

Generally speaking, the CM filter is a common-terminal four-port network. However, due to the symmetry of the CM filter, it can be treated as a simple passive two-port network. The DM filter is a passive two-port network. Fig. 4-2 shows how a typical EMI filter is decomposed into two (CM and DM) two-port networks. The DM part is obtained by leaving the ground terminals open while the CM part is obtained by shorting the Line and Neutral terminals on both sides. As a convention, the port facing the noise source is to be called Port #1 and the port facing the noise load (such as LISN's) is to be called Port #2. Thus, for either the CM or the DM filter, a 4×4 matrix can be

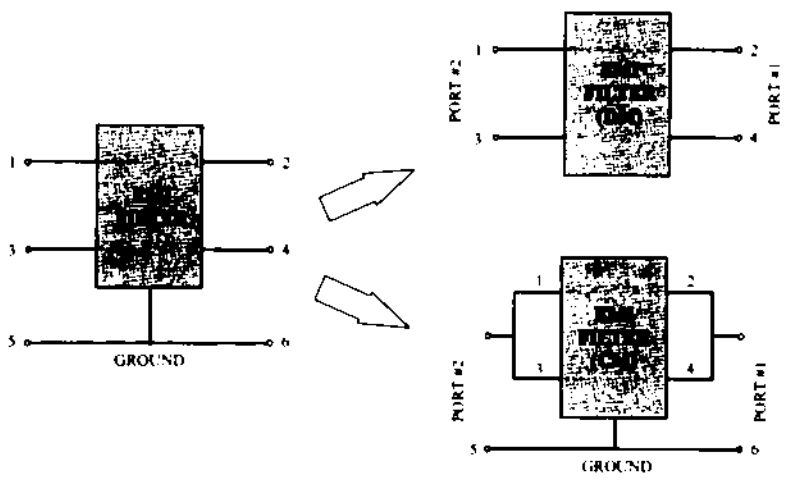

Fig. 4-2 Decomposition of an EMI Filter into CM and DM Parts

employed to describe it. Furthermore, since the filter is usually made up of LCR's, it is a reciprocal network. Thus the elements *12* and *21* of the 4×4 matrix should equal (e.g. $Z_{12} = Z_{21}$), leaving only three unknown parameters for a complete description of a filter.

Filter attenuation (or insertion loss) is defined as the ratio of the load voltage without the filter to that with the filter (*see* Eq.(5) on page 23). If the source and load impedance plus the filter describing matrix parameters are known, attenuation can be calculated. Now the problem is which matrix to choose. The selection criterion is ease of measurement and ease of usage.

4.2 A Proposed Characterization Method For EMI Filters

A two port [Z] matrix $\begin{bmatrix} Z_{11} & Z_{12} \\ Z_{21} & Z_{22} \end{bmatrix}$ is proposed for the characterization of an EMI filter. The [Z] matrix is chosen for the reason that all the four parameters can either be measured or calculated from simple measurement. The details are given in the following paragraphs.

Both Z_{11} and Z_{22} are driving point impedance and can be measured quite accurately up to very high frequencies (e.g. 30MHz) using an impedance analyzer. The transfer impedance Z_{12} and Z_{21} are not easily measurable as explained in Section 4.1. Fortunately, most EMI filters can be treated as a passive reciprocal network, so $Z_{12} = Z_{21}$ (in the situation of an active EMI filter, the statement may not hold). Let the symbol Z_T

be used to represent the transfer impedance, i.e., $Z_{12} = Z_{21} = Z_T$. So now there is only one transfer impedance to determine. One measurement that is both easy to carry out and closely related to transfer impedance is the measurement of filter attenuation in a known system (typically a 50Ω system). For example, the gain-phase analyzer function of an HP4194A (*see* Fig. 4-5) enables the measurement of the complex attenuation of a two-port filter in a 50Ω system. This may be used to determine Z_T. A look at the mathematics will give us a clearer view of the relationship. Fig. 4-3 shows the intended use of the filter. The relationship between filter attenuation and its impedance matrix can be determined in the following manner.

Relationship among the four port variables (from definition of [Z] matrix):

$$\begin{bmatrix} V_1 \\ V_2 \end{bmatrix} = \begin{bmatrix} Z_{11} & Z_T \\ Z_T & Z_{22} \end{bmatrix} \cdot \begin{bmatrix} I_1 \\ I_2 \end{bmatrix} \qquad (18)$$

Relationship between port variables and external circuit:

$$V_1 = V_S - Z_S \cdot I_1 \qquad (19)$$

$$V_2 = -Z_L \cdot I_2 \qquad (20)$$

By definition (*see* Eq.(5) on page 23), the attenuation of the filter is:

$$A_T = \frac{\dfrac{Z_L}{Z_L + Z_S} \cdot V_S}{V_2} \qquad (21)$$

By manipulating Eq.(18) through Eq.(21) above, the following expression can be obtained:

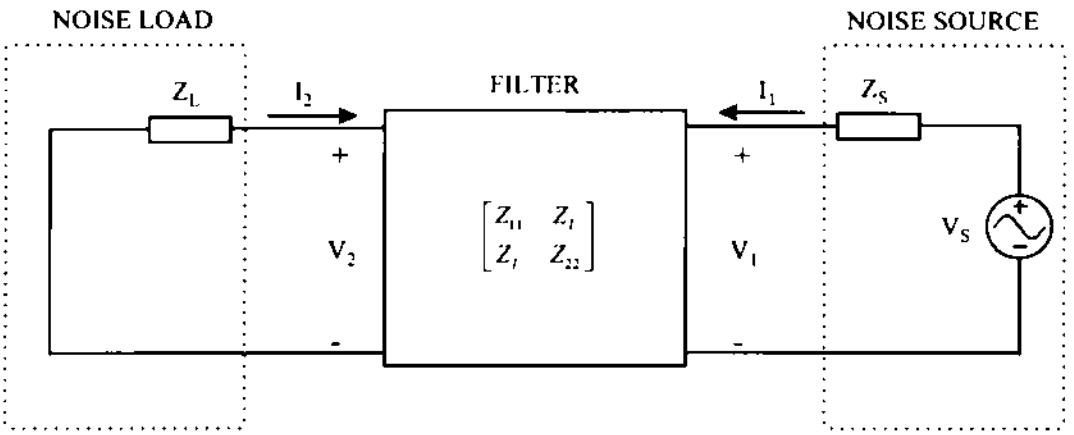

Fig. 4-3 Relationship Between Filter [Z] Matrix and Filter Attenuation

$$A_I = \frac{Z_S Z_I + Z_I Z_{11} + Z_S Z_{22} + Z_{11} Z_{22} - Z_T^2}{Z_T (Z_S + Z_L)} \qquad (22)$$

Or alternatively,

$$Z_T^2 + Z_T A_I (Z_S + Z_L) = Z_S Z_L + Z_L Z_{11} + Z_S Z_{22} + Z_{11} Z_{22} \qquad (23)$$

This is a quadratic equation of Z_T. If both the source and load impedance are known, and especially when they are equal (i.e., $Z_I = Z_S = R$), Eq.(23) can be simplified as:

$$Z_T^2 + Z_T A_I (2R) = R^2 + RZ_{11} + RZ_{22} + Z_{11} Z_{22} \qquad (24)$$

By solving it, we have

$$Z_T = -R \cdot A_I + \sqrt{(RA_I)^2 + R^2 + R(Z_{11} + Z_{22}) + Z_{11} Z_{22}}\,, \qquad (25)$$

where A_I is the attenuation when both the source and load impedance are equal to R. Therefore, for a given R value and the measured results of Z_{11}, Z_{22} and A_I, Z_T can be calculated according to Eq.(25). A_I can be practically measured using a gain-phase analyzer such as the HP4194A. It should be pointed out that the choice of R does not affect Z_T since A_I varies accordingly. In practice, R is usually chosen to be 50Ω.

Notice that the square root operation in Eq.(25) is performed in the complex sense, and there are two values associated with it. The magnitudes of the two roots of Z_T are very different, one being very large, the other very small. In the context of a low pass filter such as the EMI filter, a low value of Z_T is the reasonable choice.

Notice that all the [Z] parameters and A_I discussed here are complex variables and are functions of frequency. One of the advantages of using this approach is that all

parasitic effects are automatically included in the characteristics.

4.2.1 *Characterization Matrices For Common Mode And Differential Mode*

For a given filter, there is a corresponding set of $[Z]_{CM}$ parameters, i.e. Z_{11}, Z_{22} and Z_T for the common mode characteristics and a set of $[Z]_{DM}$ parameters for the differential mode characteristics. In other words, it takes two sets of [Z] parameters to completely characterize a composite EMI filter.

4.2.2 *Usage Of The Filter [Z] Matrix*

With a known [Z] matrix, one can predict the attenuation of an EMI filter when the noise source impedance and noise load impedance are given. To find out the filter attenuation with a specific source impedance and load impedance, the following equation can be used:

$$|A_T| = \left| \frac{Z_S Z_L + Z_L Z_{11} + Z_S Z_{22} + Z_{11} Z_{22} - Z_T^2}{Z_T (Z_S + Z_L)} \right| \qquad (26)$$

where Z_S is the source impedance and Z_L is the load impedance. This equation comes directly from Eq.(22). It is noted that all the parameters, Z_s, Z_L, Z_{11}, Z_{22}, Z_T are complex numbers in general.

4.3 Experimental Verification

To verify the proposed method, an off-line power supply was used as the noise source and a commercial EMI filter as the device under test (DUT below). Schematic of the DUT is shown in Fig. 4-4.

In Section 4.3.1, actual implementation will be described and the results will be shown. In Section 4.3.2, a comparison of the predicted and the measured results is given.

4.3.1 Experimental Characterization of the Filter

The measurement of Z_{11} and Z_{22} is straightforward: by using an impedance measuring equipment such as the HP4194A (*see* Fig. 4-5), Bode plots of the impedance can be directly obtained. Fig. 4-6(a) and (b) show the plots of the complex Z_{11} and Z_{22} of the DM part of the DUT.

The setup shown in Fig. 4-5 is for measurement of A_T in a 50Ω system. A sinewave signal is generated by a built-in 50Ω source and is split into two identical signals (at the two channels marked 'DUAL') by a built-in power splitter. One signal is directed to the REFERENCE channel, the other is fed to the input of the DUT. The signal going through the DUT is attenuated by it and then sent to the TEST channel. Due to the function of the power splitter, the two signal paths are well isolated and therefore the signal at the REFERENCE channel is equal to the signal that would appear at the

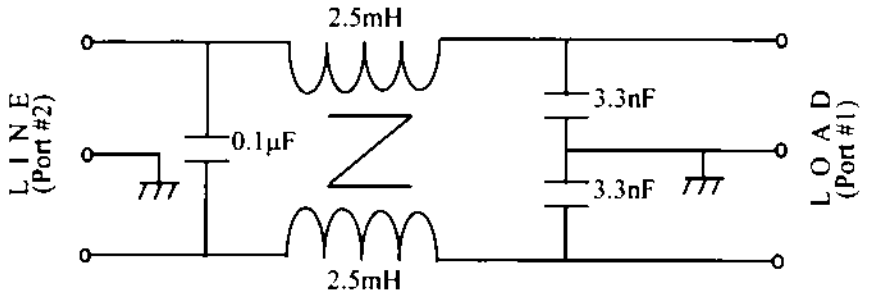

Fig. 4-4 Schematic of a Commercial EMI Filter (Delta 03GEEG3H)

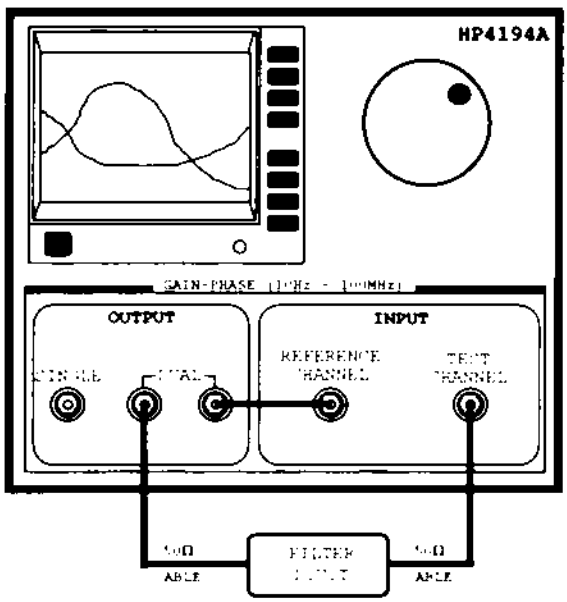

Fig. 4-5 Setup for Measuring Filter Attenuation A_T in a 50Ω System

TEST channel when there is no filter. Therefore the ratio of the signal at the REFERENCE channel to that at the TEST channel is the filter attenuation. The measured A_T curves of the DM part of the DUT are shown in Fig. 4-6(c). By using the results of Fig. 4-6(a), (b), (c) and Eq.(25), Z_T can be obtained. See Fig. 4-6(d).

The results shown in Fig. 4-6(a) (Z_{11}), (b) (Z_{22}) and (d) (Z_{12} and Z_{21}) are a complete representation of the DUT's DM characteristics. For example, the [Z] matrix at 1.1MHz is as follows (from the figure):

$$\begin{bmatrix} Z_{11} & Z_{12} \\ Z_{21} & Z_{22} \end{bmatrix}_{DM} = \begin{bmatrix} 65\angle 76° & 2.9\angle -180° \\ 2.9\angle -180° & 1.2\angle -86° \end{bmatrix}. \qquad (27)$$

As frequency varies, [Z] matrix changes according to these figures.

CM characteristics can be obtained in like manner and the results are shown in Fig. 4-7.

4.3.2 *Verification of Filter Attenuation in an Experimental Power Supply*

By using the filter characteristics curves obtained (*see* Fig. 4-6 and Fig. 4-7), filter effectiveness can be predicted for a specific power supply. The noise source impedance of the power supply was measured using the insertion loss method discussed in Chapter III, and the results are shown in Fig. 4-8. By using Eq.(26) in Section 4.2.2 and the results in Fig. 4-6, Fig. 4-7 and Fig. 4-8, filter attenuation can be calculated. The predicted and the measured attenuation curves are shown in Fig. 4-9. For both DM and CM, the predicted and the measured curves agree very well.

4.3.3 Discussion

In Fig. 4-9, attenuation in a 50Ω system is also shown (dotted lines). Although the difference between the attenuation in two different type of systems (i.e. a 50Ω system and a non-50Ω system) is not significant in this example, there exist situations where the difference is much more significant. This happens when either the noise source or noise load impedance or both deviate significantly from 50Ω. Fig. 4-10 shows the DM attenuation of the DUT under different source and load impedance conditions. Notice for Curve#2 where "FCC" is indicated, the noise load is 100Ω, and for Curve#3 and Curve#4 where "MIL-STD-461B" is indicated, two standard 10μF feedthrough capacitors are used (in series) as the noise load. The notation "$|Z_{sdm}|$ = 47nF" means the DM source impedance is approximately that of a 47nF capacitor.

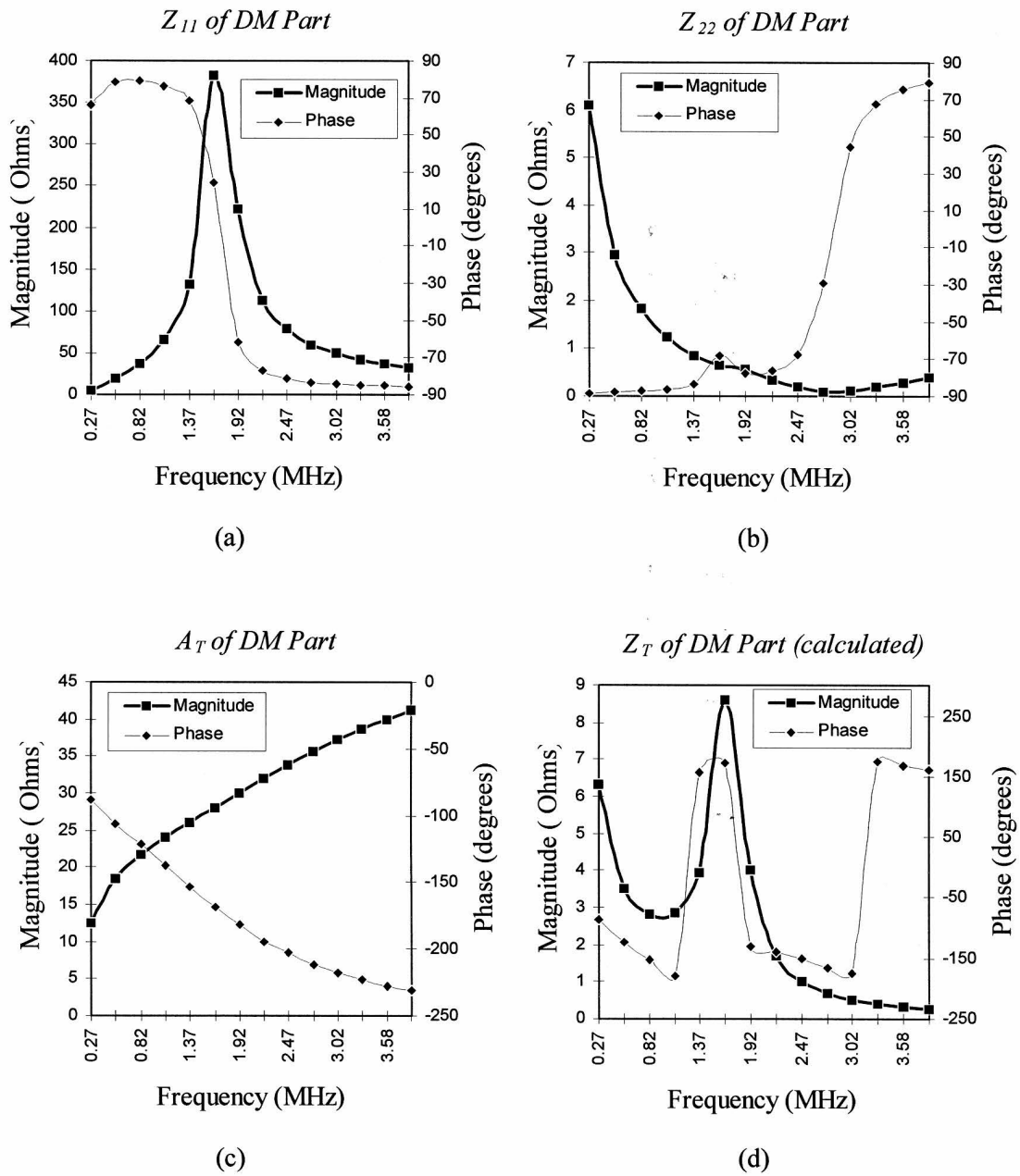

Fig. 4-6 [Z] Parameters of the DM Part of the Filter Shown in Fig. 4-4

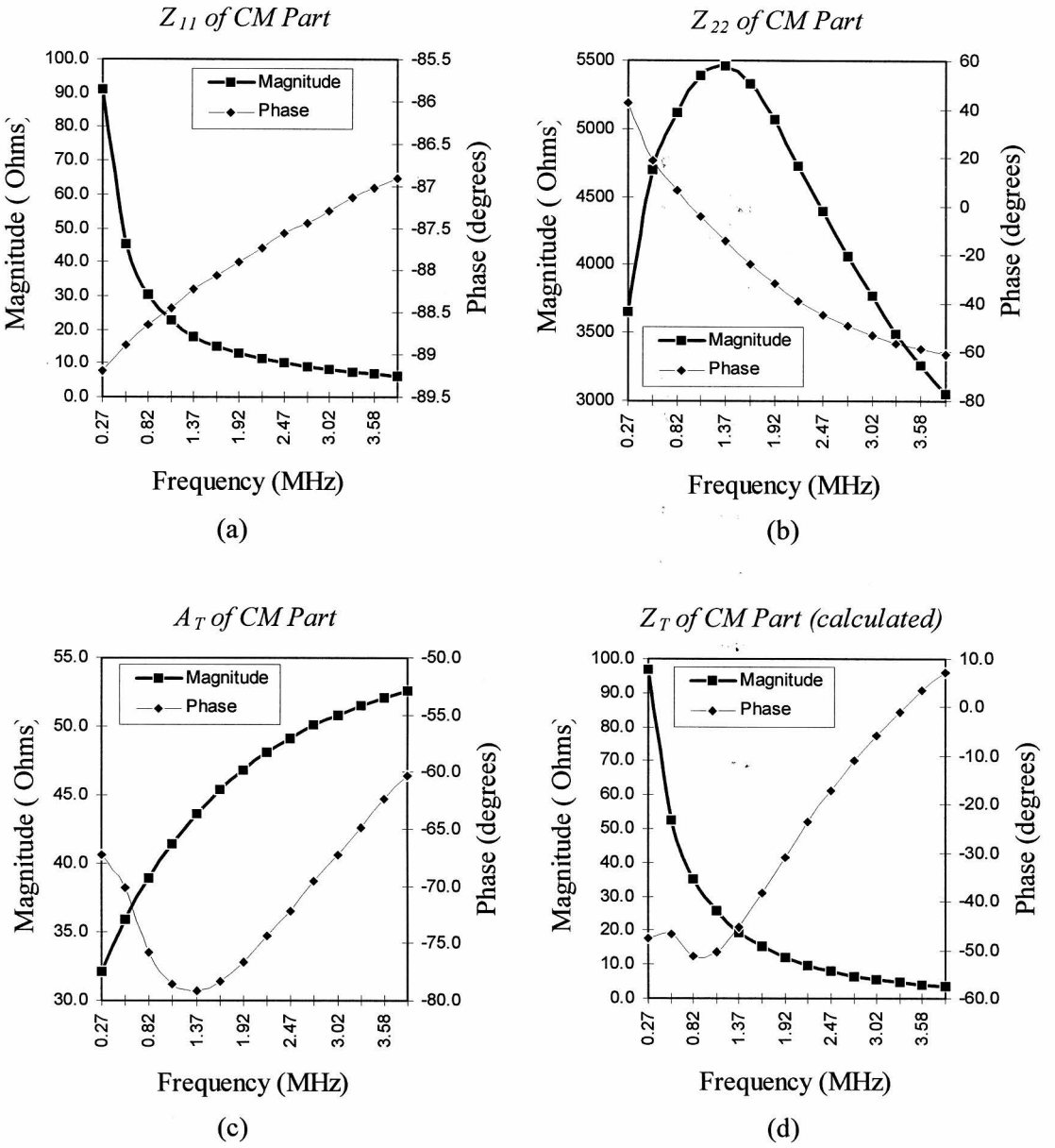

Fig. 4-7 [Z] Parameters of the CM Part of the Filter Shown in Fig. 4-4

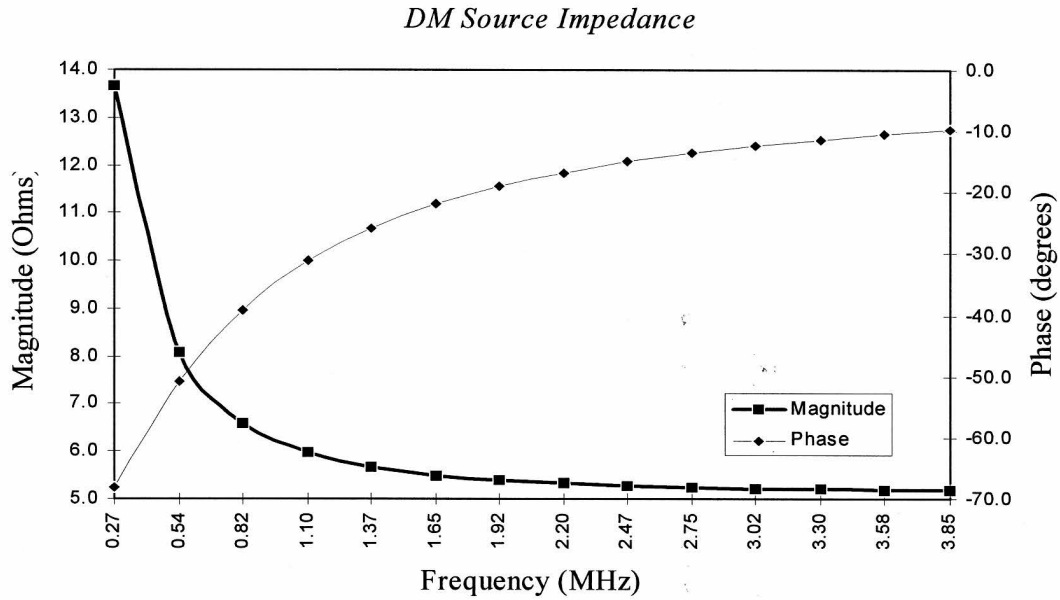

(a)

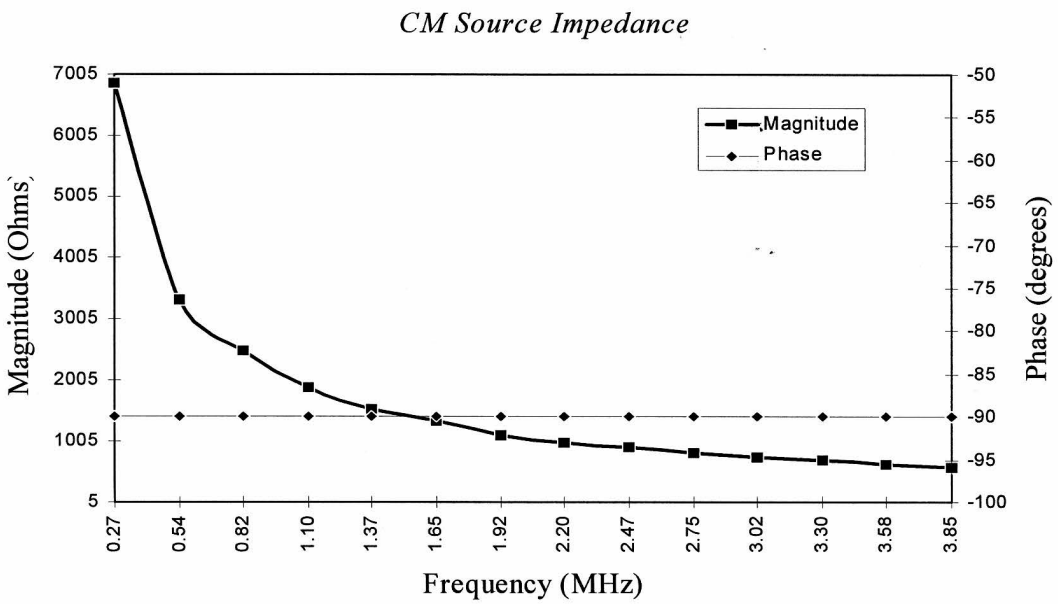

(b)

Fig. 4-8 Noise Source Impedance of the DUT
(a) DM (b) CM

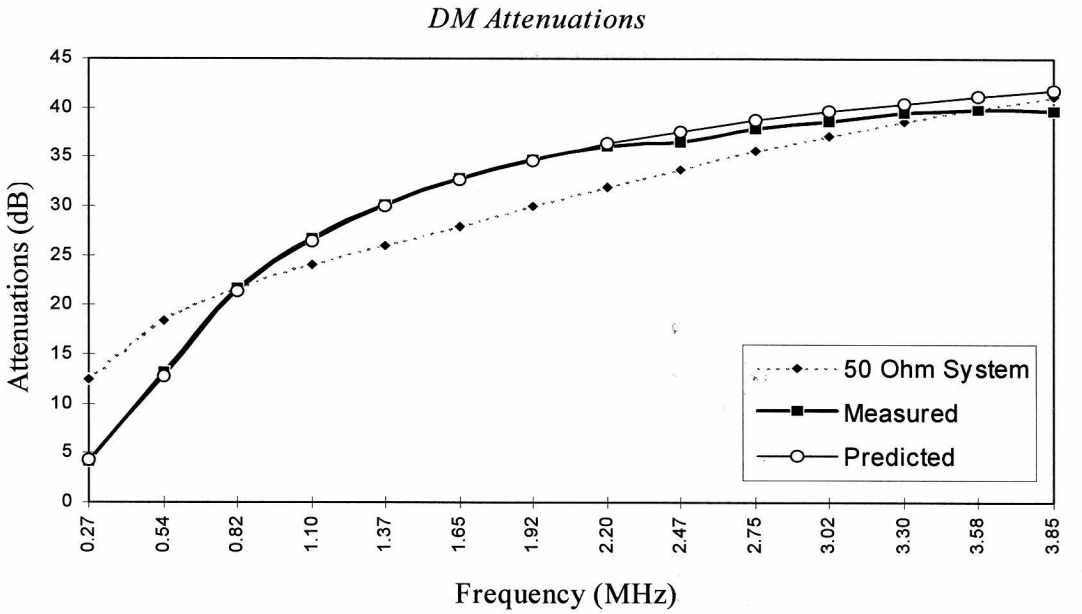

(a)

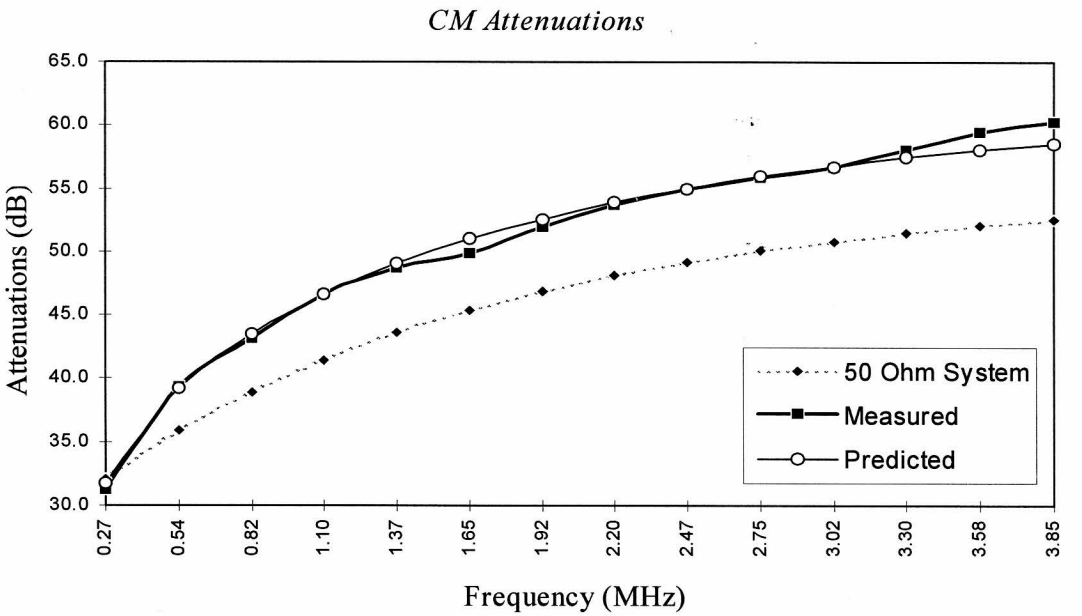

(b)

Fig. 4-9 Measured Attenuation Vs. Attenuation Predicted By [Z] Matrix
(a) DM (b) CM

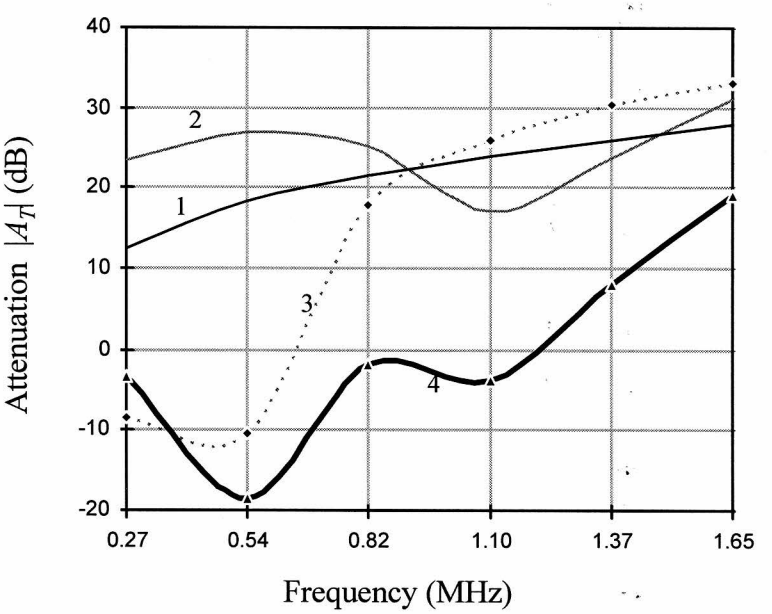

1. Z_{sdm}=50Ω, 50Ω load
2. $|Z_{sdm}|$ = 1.7nF, FCC LISN
3. $|Z_{sdm}|$ = 47nF, MIL-STD-461B
4. $|Z_{sdm}|$ = 1.7nF, MIL-STD-461B

Fig. 4-10 DM Attenuation of the DUT Under Different Source and Load Impedance Conditions

Chapter V

CONCLUSIONS AND FUTURE RESEARCH

5.1 Conclusions

Several conclusions are summarized in the following.

1. The Insertion Loss Method has been found very effective both in investigating conducted emission mechanisms and in the actual measurement of the noise source impedance.

Insertion Loss Method only measures the magnitude of source impedance. When necessary, the Hilbert transform can be used to derive approximate phase information of the source impedance from the magnitude curve.

2. The measurement of the noise source impedance of an off-line converter is much more complicated than dc/dc converter source impedance measuring. Noise emission mechanisms has to be first recognized, or the measurement result can be useless. For an experimental off-line converter, noise emission mechanism when the diode bridge is off has been found very different from that when the diode bridge is on. The severe unbalance in the circuit during diode bridge OFF time introduces huge DM noise. It is concluded that only the source impedance during diode bridge ON time is of practical importance.

3. It is found that in an off-line power supply, because the emissions are usually modulated by the rectifier, zero-span mode of the spectrum analyzer is the desirable mode of operation to observe the time-varying nature of the emission. Insight into emission nature is obtained through this mode of operation.

4 The proposed Signal Injection Method to measure source impedance is a good method in that it directly provides the phase information as well as magnitude information of the measured impedance. A potential problem with the Signal Injection Method is, in the case of an off-line converter, the source impedance is modulated, and the measuring equipment may not respond fast enough to catch the on-off nature of the emission.

5. Impedance matrix method is proposed to characterize EMI filters. With this new characterization method and the source impedance information obtained, one can predict the filter attenuation when the filter is placed with a switching power supply. This has not been possible before. This assertion has been experimentally verified.

5.2 Future Research

1. The Signal Injection Method is a quick and easy way to measure impedance. It also provides the phase information directly. The problem is, a gain-phase analyzer such as the HP4194A may not be fast enough to accurately capture the highly changing impedance in the case of off-line power supplies where diodes are switching. Further work is necessary to resolve this problem.

2. Further work is desirable to achieve an automated system for noise source impedance measurement and an automated system for characterizing the filter attenuation.

3. With the systems described in Item #2, it is desirable to integrate this system with software to automate the design of an EMI filter for power supplies.

REFERENCES

[1] Lon M. Schneider, *Noise Source Equivalent Circuit Model for Off-line Converters and Its Use in Input Filter Design*, Proceedings of Powercon 10, 1982.

[2] Ting Guo, *Separation of the Common-Mode and the Differential-Mode Conducted Electromagnetic Interference Noise*, Master's Thesis, Virginia Polytechnic Institute and State University, 1994

[3] Morris Engelson, *Modern Spectrum Analyzer Measurements*, JMS, 1991.

[4] Frederic M. Tesche, *On the Use of the Hilbert Transform for Processing Measured CW Data*, IEEE Transactions on Electromagnetic Compatibility, Vol. 34, No.3, August 1992.

[5] Norman Balabanian and Theodore A. Bickart, *Linear Network Theory*, Matrix, 1981.

The vita has been removed from the scanned document